Electronic Supplementary Information for

Excitation wavelength-dependent multi-coloured and white-light emissive pyrene-based hydrazones: suppression of Kasha's rule

Naveen Kumar M,[a] Deikrisha Lyngdoh Lyngkhoi,[b] Sudhakar Gaikwad,[c] Jayanta Samanta,[a] Rafiq Ahamed,[c] Snehadrinarayan Khatua,*[b] and Susnata Pramanik*[a]

[a]Department of Chemistry, Faculty of Engineering and Technology, SRM Institute of Science and Technology, Kattankulathur, 603203 India. E-mail: susmatap@srmist.edu.in

[b]Centre for Advanced Studies, Department of Chemistry, North-Eastern Hill University Shillong, Meghalaya 793022, India. E-mail: snehadri@gmail.com; skhatua@nehu.ac.in

[c]Division of Organic Chemistry, CSIR-National Chemical Laboratory, Dr. Homi Bhabha Road, Pashan, 411 008, Pune, Maharashtra, India.

Contents

1. General Information

Chemicals were bought from Avra, SRL and Carbanio and used without purification. Thin Layer Chromatography was carried out under TLC Silica gel 60 RP – 18 F_{254s}. NMR spectra were recorded on a Bruker 500 MHz NMR spectrometer. In NMR, the multiplicities of the signals are presented as s: singlet, d: doublet, m: multiplet, dd: doublet of doublets, and t: triplet. Deuterated solvents are used as a reference using the residual solvent peak and as the internal standard. ESI-HRMS data were collected in LC/MS, 6230B Time of Flight (TOF) Agilent Technologies and QTOF-ESI source M/S Bruker Daltonik GmbH, Germany. UV studies were carried out in Shimadzu UV3600+ and Agilent using HPLC grade solvents. Fluorescence studies were conducted in Edinburg instruments FLS 1000 and Horiba – Jobin – Yvon Fluorolog FL3-111. The intensity for the solid-state fluorescence was normalized. Single crystal XRD analysis was carried out in Bruker D8 quest x-ray diffractometer with MoKα (λ = 0.71073) radiation.

2. Synthesis of hydrazones

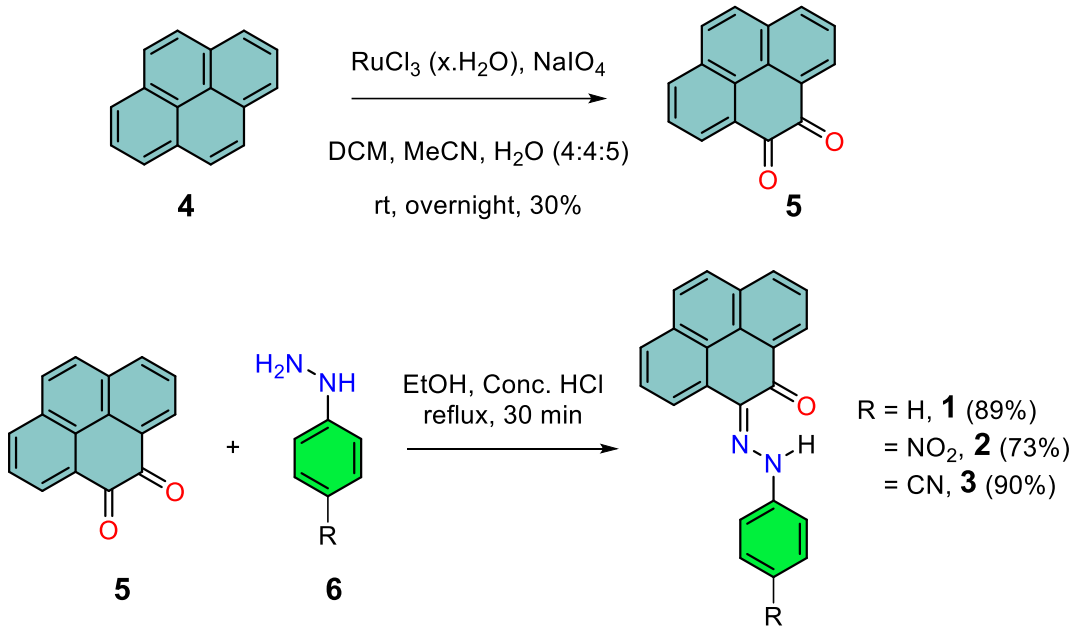

Scheme S1. Synthetic scheme of pyrene-based hydrazones

2.1 Synthetic procedure for 4,5-Pyrenedione

Pyrenedione was prepared according to the reported procedure,[1] pyrene (1 equiv.), $RuCl_3$ (x.H_2O) (0.1 equiv.) and $NaIO_4$ (4 equiv.) were taken in a mixture of dichloromethane (40 mL), acetonitrile (40mL) and distilled water (50 mL) in a Round bottom flask. After stirring the mixture at room temperature for overnight organic solvents were removed under reduced pressure and extracted with DCM (3×50 mL). Organic layer was dried over Na_2SO_4 and removed under reduced pressure. Finally, the product was purified by silica gel column chromatography using 60% DCM in hexane (30% yields).

2.2 General procedure for pyrene-hydrazones[2]

In a round bottom flask, 4,5-pyrenedione (1 equiv.), hydrazine hydrochloride (1 equiv.), Conc. HCl (0.5 mL) and ethanol (10 mL) were taken, and the mixture was refluxed for half an hour (the progress of the reaction was checked using TLC). The reaction mixture was then cooled to room temperature and the precipitates were filtered and washed with cold ethanol for three times (3 × 5 mL). Finally, they were recrystallized from methanol leading to the target hydrazones **1-3**. All the compounds were prepared around 350 mg scale.

1: (Yield: 90%). ^{1}H NMR (500 MHz, $CDCl_3$) δ 16.18 (s, 1H), 8.72 – 8.60 (m, 2H), 8.18 (d, *J* = 8.0 Hz, 1H), 7.91 – 7.78 (m, 5H), 7.69 – 7.63 (m, 2H), 7.47 (t, *J* = 7.5 Hz, 2H), 7.21 (t, *J* = 7.5 Hz, 1H).^{13}C NMR (101 MHz, $CDCl_3$) δ 179.7, 142.6, 132.3, 131.5, 131.4, 131.3, 129.9, 129.6, 129.3, 128.8, 127.7, 127.3, 126.2, 126.2, 126.1, 125.8, 125.3, 122.2, 120.0, 116.5 ppm. ESI-HRMS: *m*/*z* (%) = 323.1179 ($[C_{22}H_{14}N_2O\text{-}H]^+$); calcd. *m*/*z* = 323.1184.

2: (Yield: 73%). ^{1}H NMR (500 MHz, $CDCl_3$) δ 15.87 (s, 1H), 8.69 (d, *J* = 7.5 Hz, 2 H), 8.35 (d, *J* = 8.5 Hz, 2H), 8.26 (d, *J* = 7.5 Hz, 1H), 8.01 (d, *J* = 7.5 Hz, 1H), 7.94-7.84 (m, 4H), 7.71 (d, *J* = 8.5 Hz, 2H) ppm. NB: ^{13}C spectrum was not able to collect due to solubility issue. ESI-HRMS: *m*/*z* (%) = 390.0850 ($[C_{22}H_{13}N_3O_3\text{-}Na]^+$); calcd. *m*/*z* = 390.0856.

3: (Yield: 90%). ^{1}H NMR (500 MHz, $CDCl_3$) *δ* 15.87 (s, 1H), 8.70 (t, *J* = 7.5 Hz, 2H), 8.34 (d, *J* = 9.5 Hz, 2H), 8.26 (d, *J* = 7.5 Hz, 1H), 8.00 (d, *J* = 7 Hz, 1H), 7.94-7.84 (m, 4H), 7.70 (d, *J* = 8.0 Hz, 2H) ppm. ^{13}C NMR (101 MHz, $CDCl_3$) δ 181.5, 146.0, 133.7, 133.4, 131.6, 131.4, 131.2, 130.7, 129.5, 128.9, 127.8, 127.5, 127.1, 126.8, 126.5, 126.3, 122.8, 120.9, 119.0, 116.1, 107.1. ppm. ESI-HRMS: *m*/*z* (%) = 348.1132 ($[C_{23}H_{13}N_3O\text{-}H]^+$); calcd. *m*/*z* = 348.1137.

3. NMR & HRMS Characterization

3.1 NMR Spectra of hydrazones 1–3

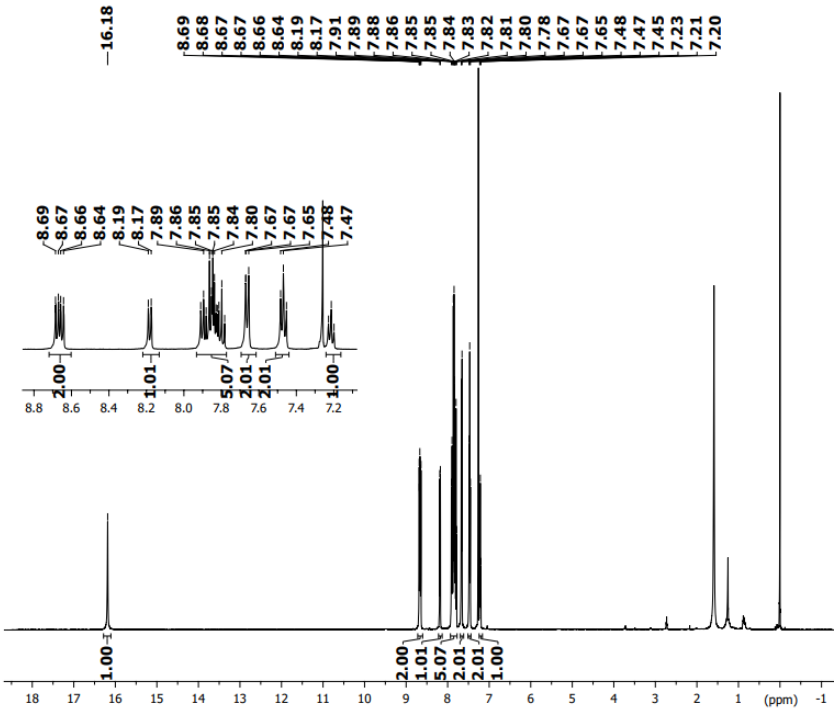

Figure S1. ^{1}H NMR (500 MHz, $CDCl_3$, 298 K) spectrum of **1.**

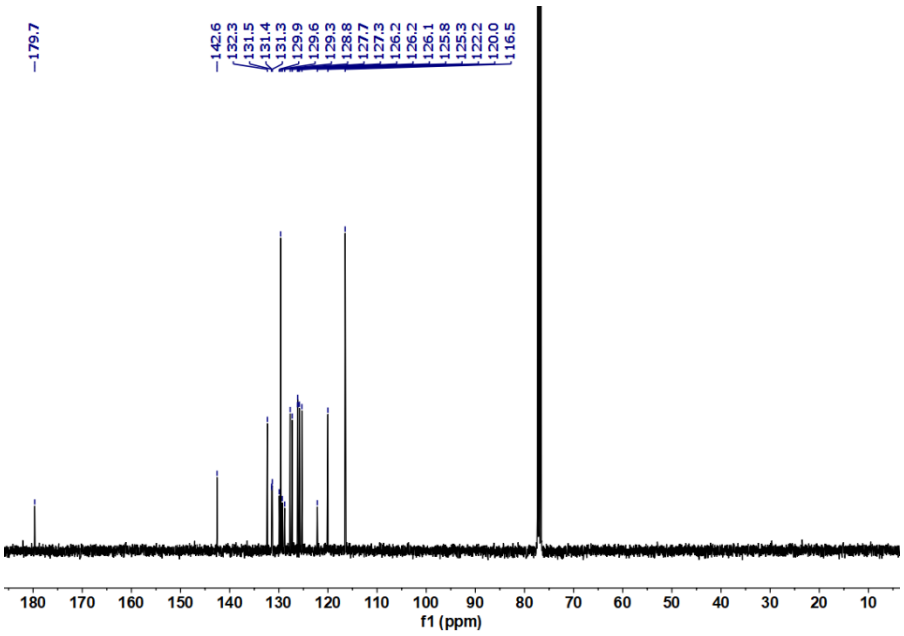

Figure S2. ^{13}C NMR (101 MHz, $CDCl_3$) spectrum of **1.**

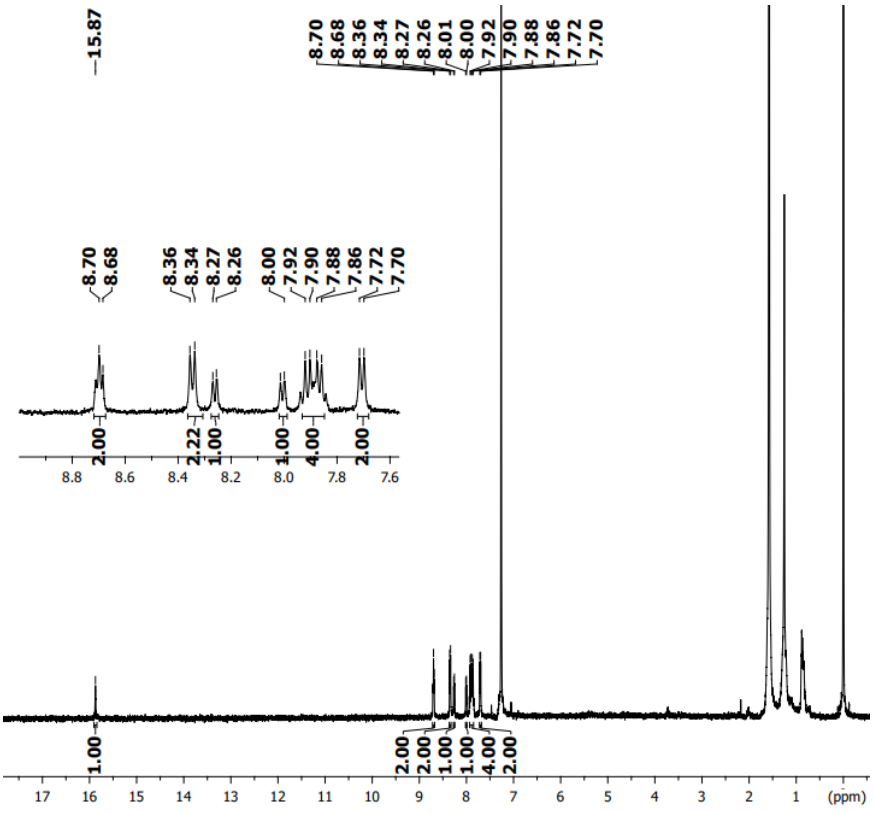

Figure S3. ^{1}H NMR (500 MHz, $CDCl_3$, 298 K) spectrum of **2.**

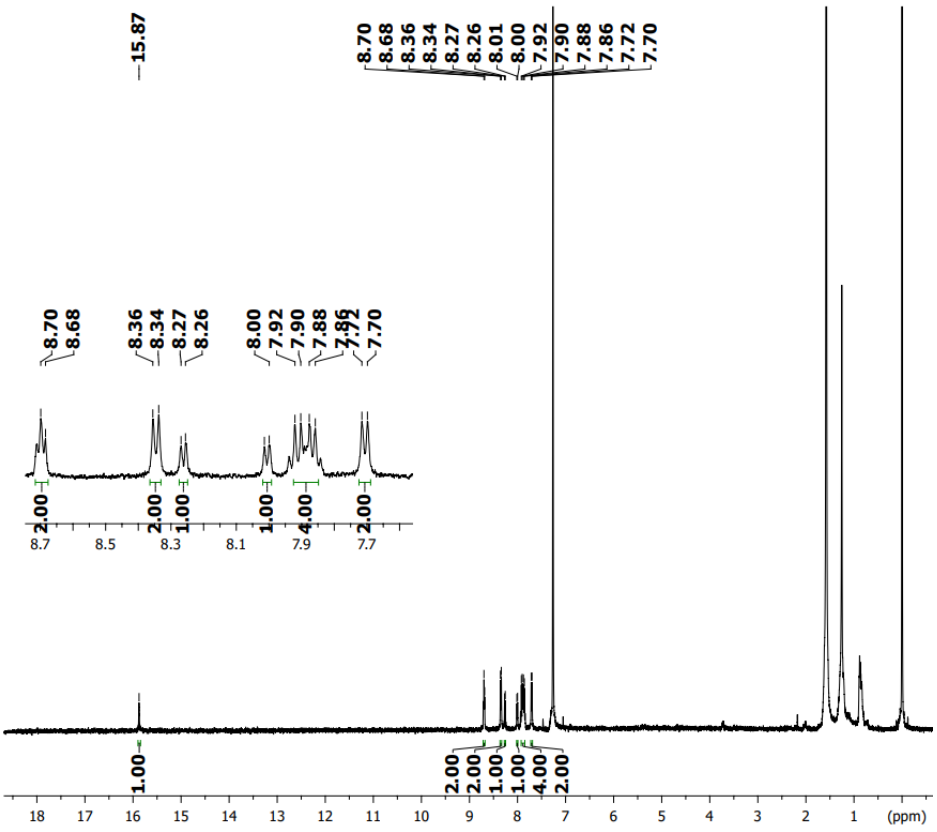

Figure S4. ^{1}H NMR (500 MHz, $CDCl_3$, 298 K) spectrum of **3.**

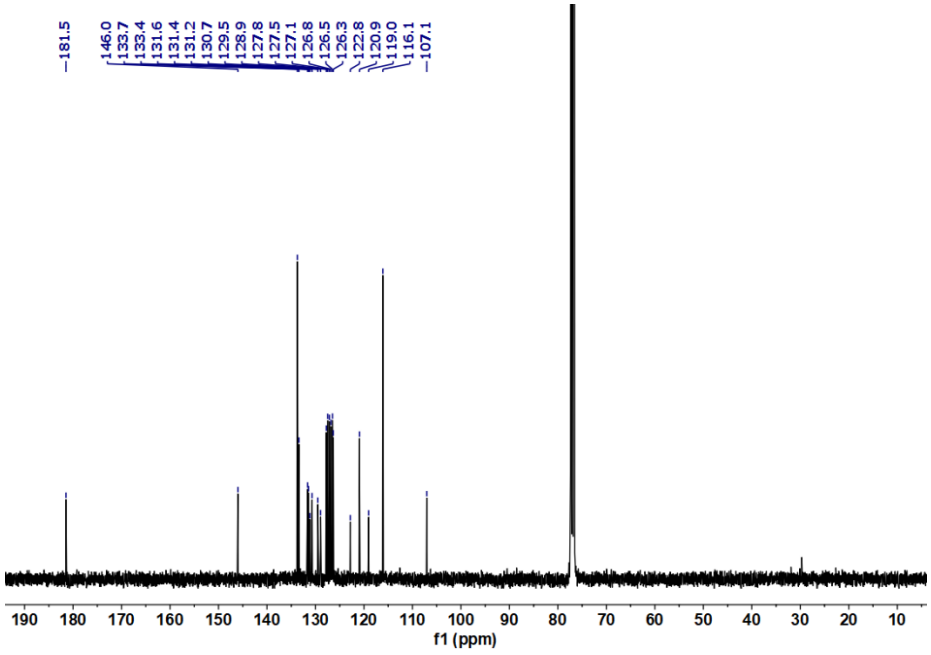

Figure S5. ^{13}C NMR (101 MHz, $CDCl_3$) spectrum of **3.**

3.2 ESI-HRMS spectra of hydrazones 1–3

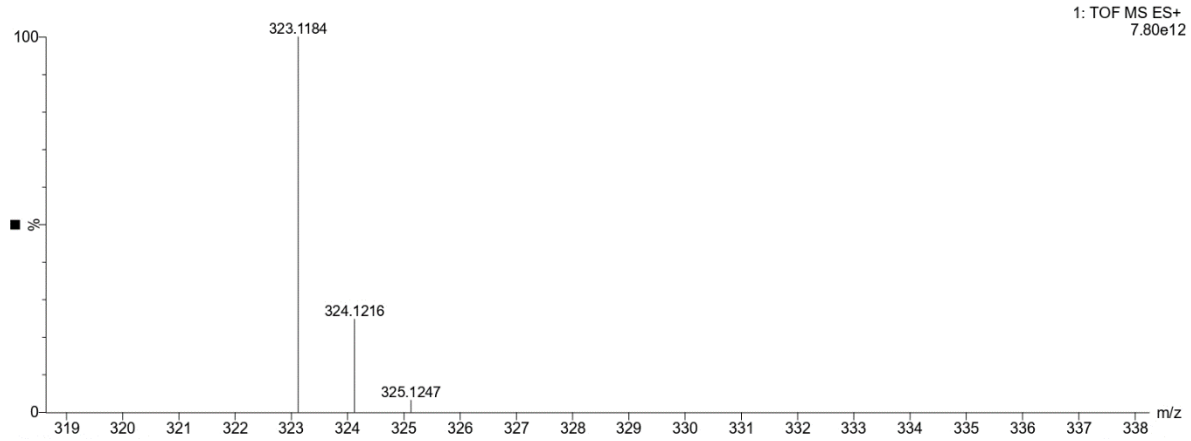

Figure S6. ESI-HRMS spectrum of **1**.

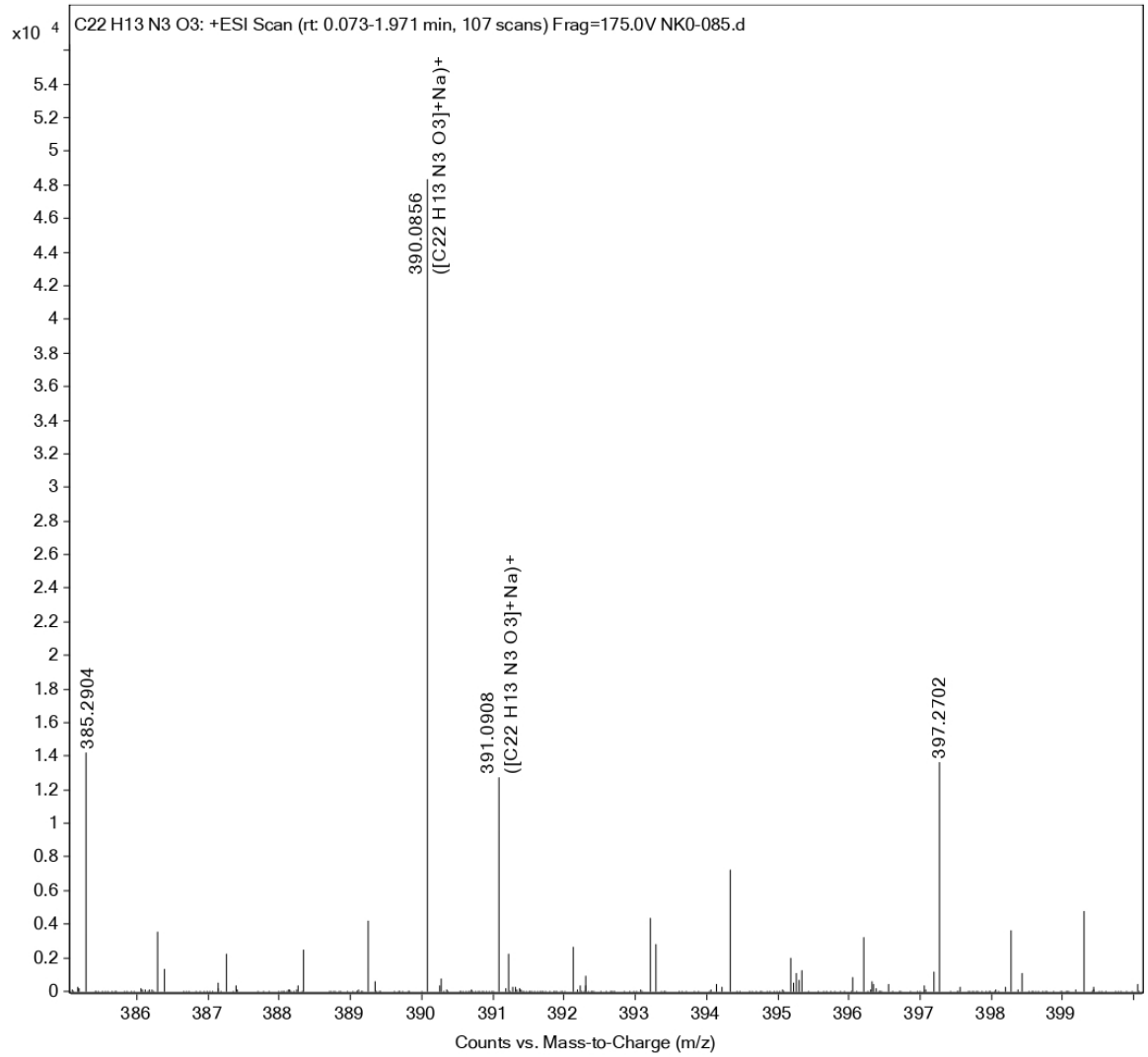

Figure S7. ESI-HRMS spectrum of **2**.

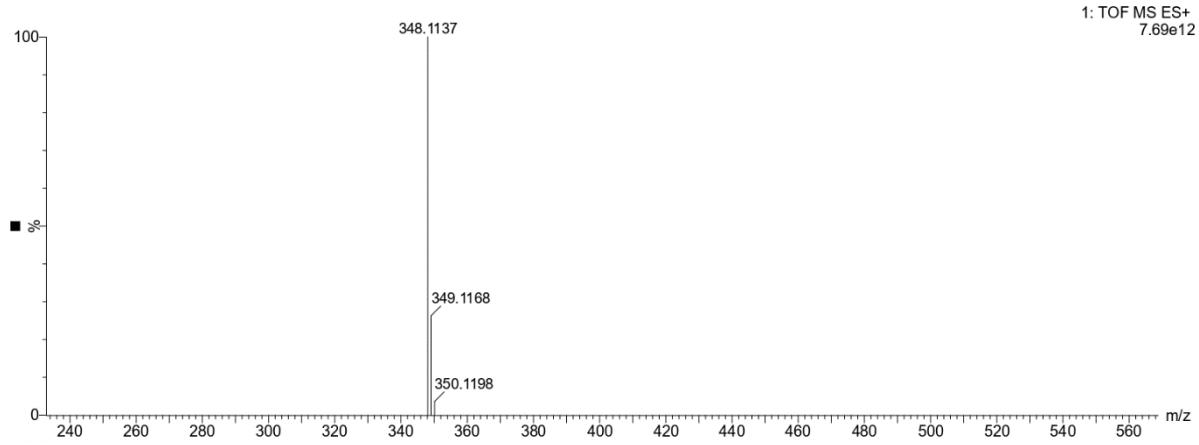

Figure S8. ESI-HRMS spectrum of **3**.

4. Photochemical studies of Pyrenedione (5)

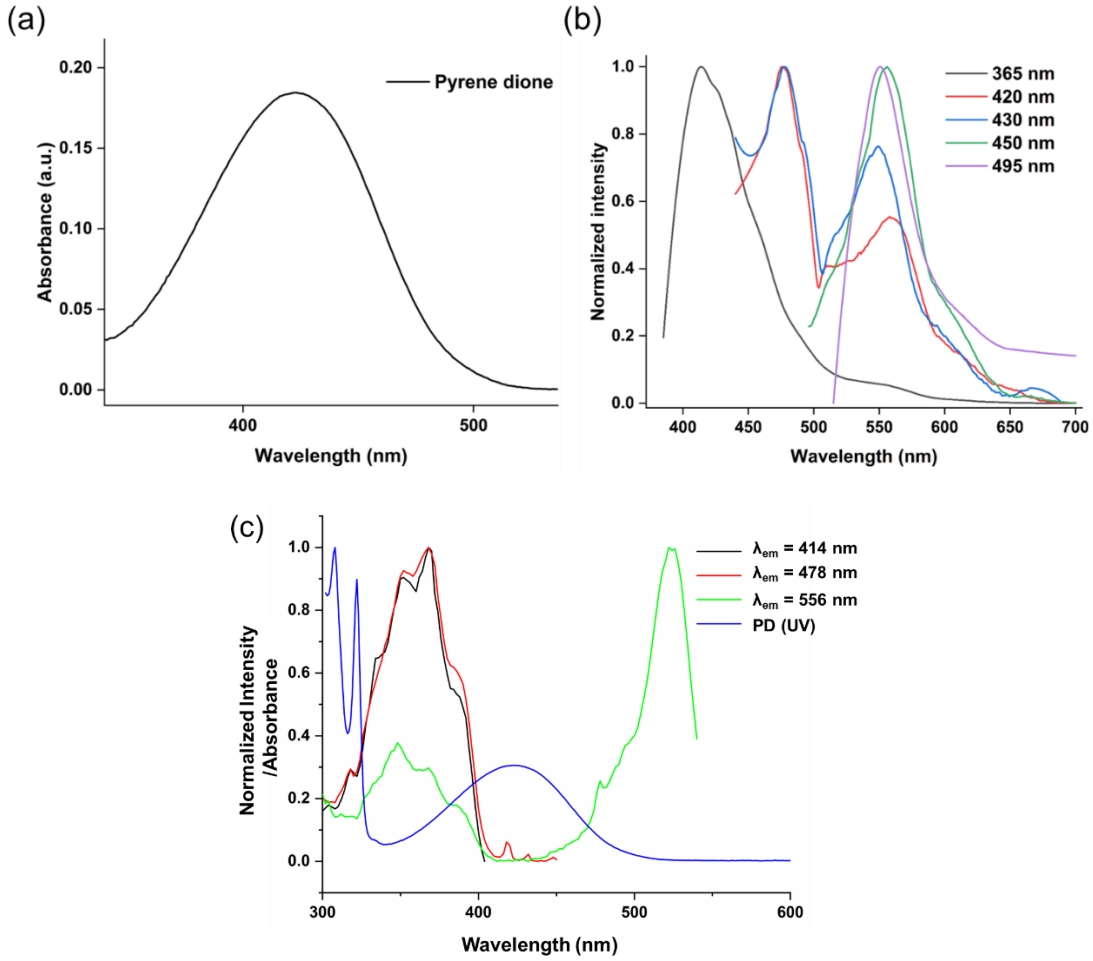

Figure S9. (a) Absorption (c = 10^{-5} M); (b) excitation wavelength-dependent emission (c = 10^{-6} M) spectra; and comparison excitation and absorption spectra of pyrenedione in MeCN at 298 K. Nearly overlapping excitation spectra for λ_{em} = 414 nm and 478 nm indicates that the emissions possibly occur from the same excited state.

5. Solution state Absorption and Fluorescence studies

5.1 Absorption spectrum of hydrazone 1–3 in different solvents

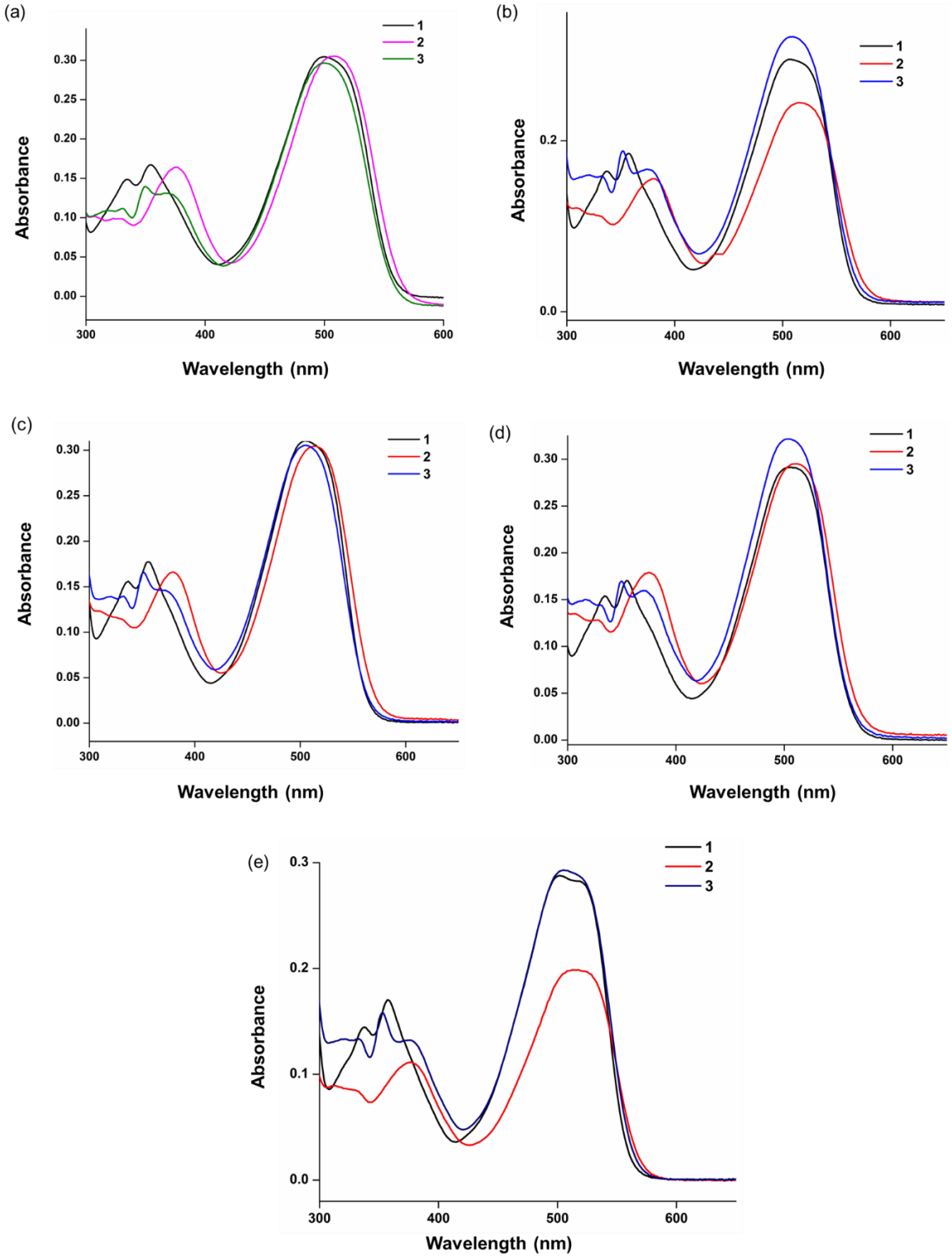

Figure S10. Absorption spectra of hydrazones **1**–**3** at 298 K in (a) acetonitrile; (b) chloroform; (c) DMF; (d) isopropanol and (e) toluene (c = 10^{-5} M).

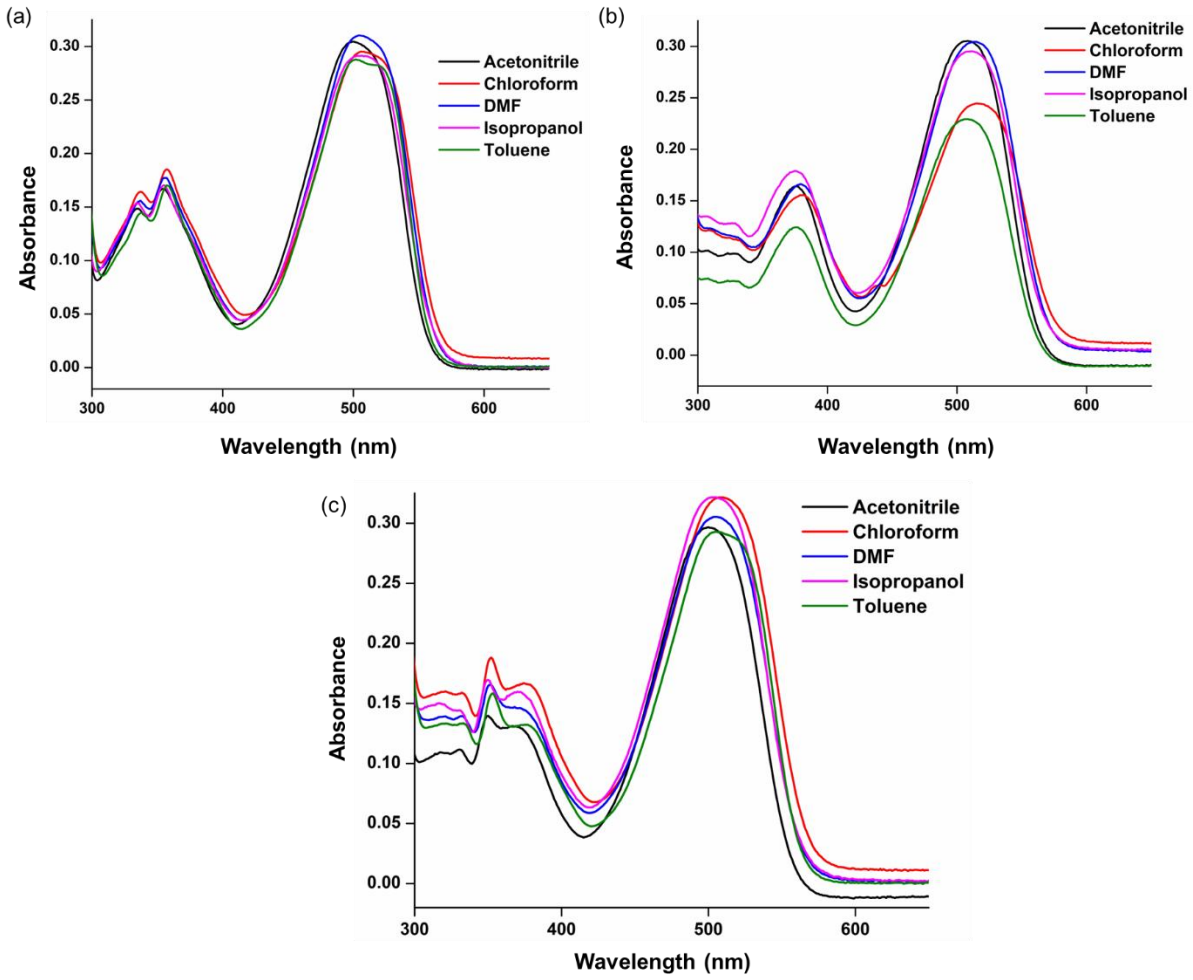

Figure S11. Absorption spectra of (a) hydrazone **1**; (b) hydrazone **2** and (c) hydrazone **3** in different solvents (c = 10^{-5} M) at 298 K.

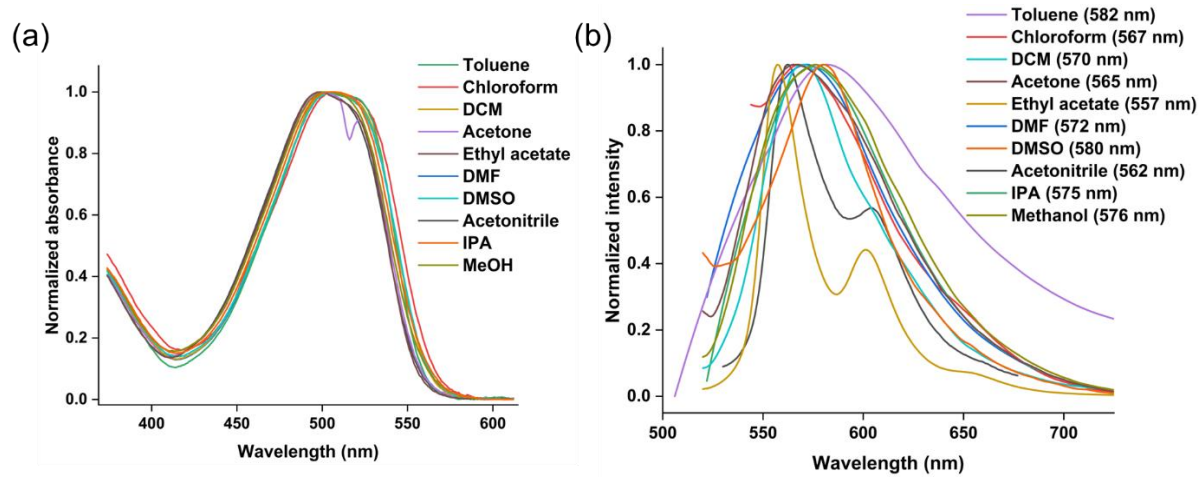

Figure S12. (a) Absorption (c = 10^{-5} M) and (b) emission (c = 10^{-6} M) spectra of hydrazone **1** in different solvents at 298 K.

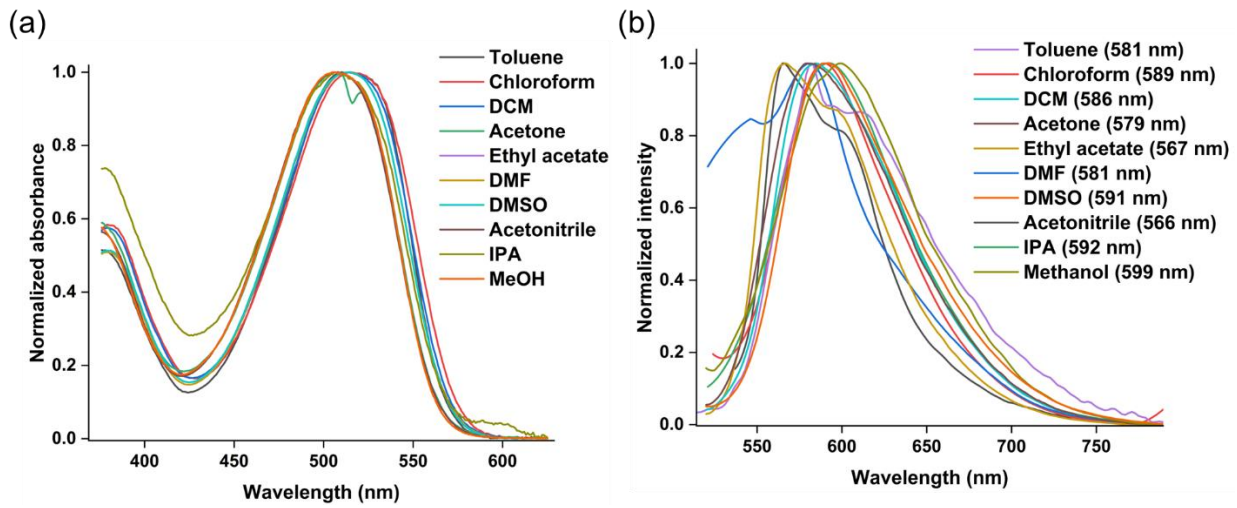

Figure S13. (a) Absorption (c = 10^{-5} M) and (b) emission (c = 10^{-6} M) spectra of hydrazone **2** in different solvents at 298 K.

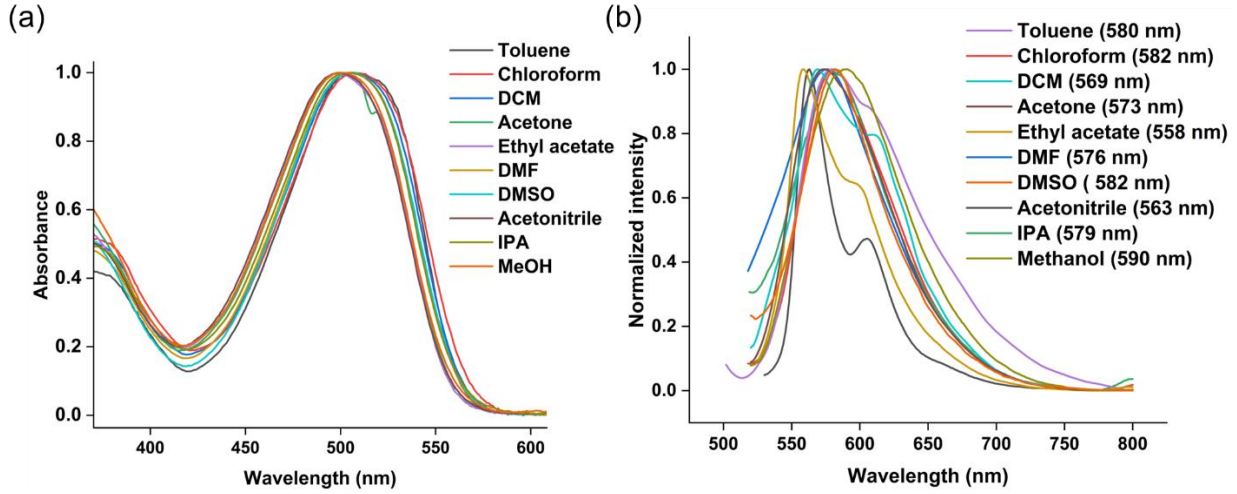

Figure S 14. (a) Absorption (c = 10^{-5} M) and (b) emission (c = 10^{-6} M) spectra of hydrazone **3** in different solvents at 298 K.

5.2 Fluorescence spectrum of hydrazone 1–3 in different solvents

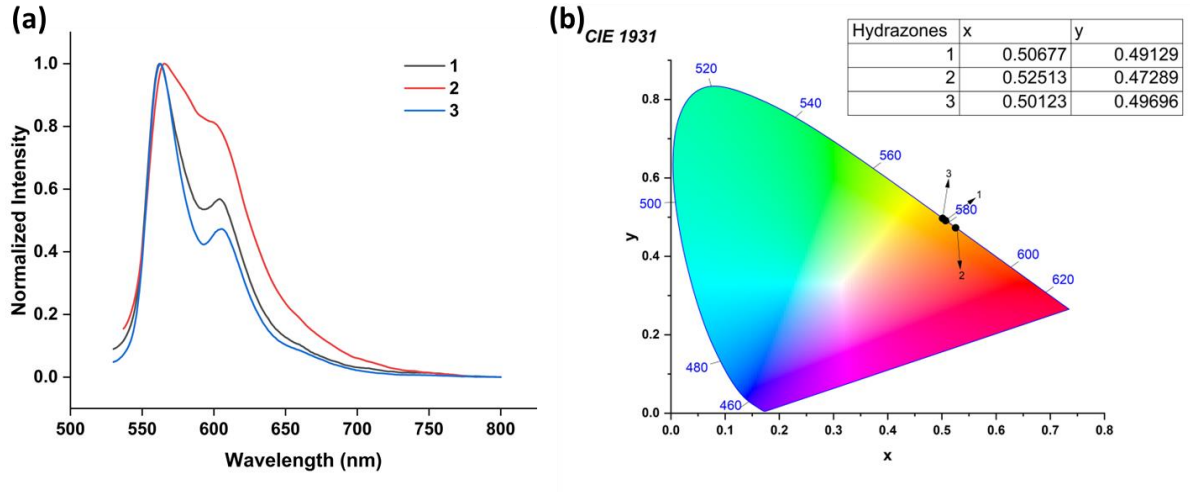

Figure S15. (a) Emission spectra (at 298 K) and (b) CIE chromaticity diagram of compounds **1**−**3** in acetonitrile (c = 10^{-6} M). Compounds **1**−**3** are excited at λ_{ex} = 496 nm, λ_{ex} = 495 nm and λ_{ex} = 492 nm, respectively.

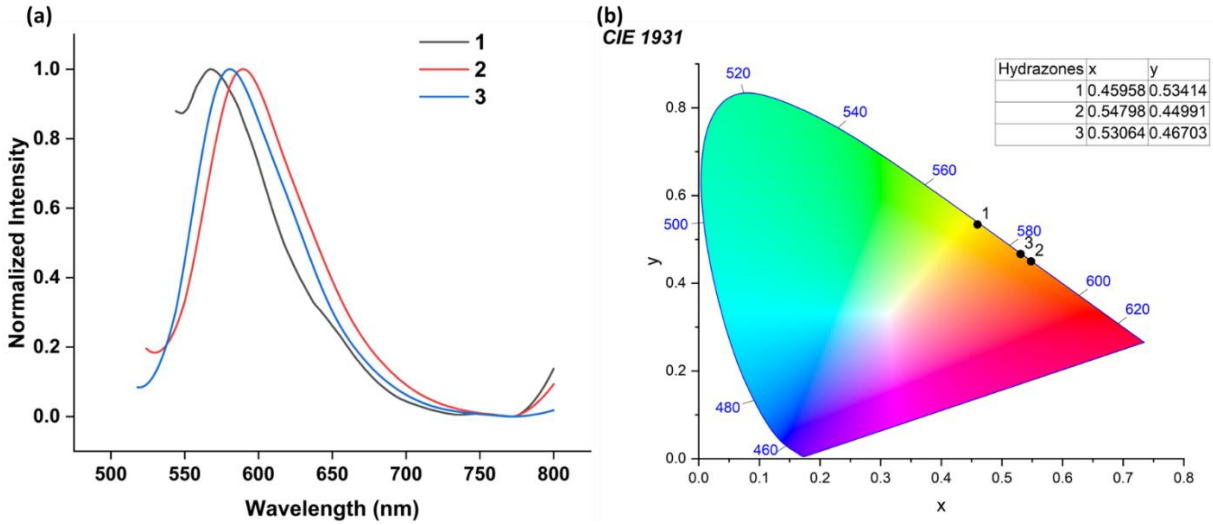

Figure S16. (a) Emission spectra (at 298 K) and (b) CIE chromaticity diagram of compounds **1**−**3** in chloroform (c = 10^{-6} M). Compounds **1**−**3** are excited at λ_{ex} = 496 nm, λ_{ex} = 495 nm and λ_{ex} = 492 nm, respectively.

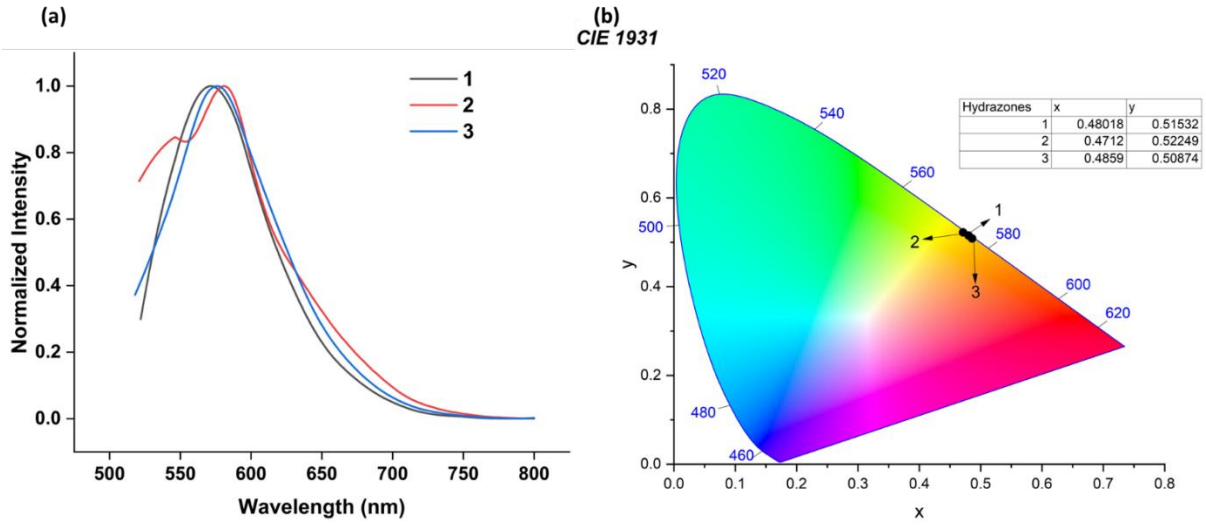

Figure S17. (a) Emission spectra (at 298 K) and (b) CIE chromaticity diagram of compounds **1**−**3** in DMF (c = 10^{-6} M). Compounds **1**−**3** are excited at λ_{ex} = 496 nm, λ_{ex} = 495 nm and λ_{ex} = 492 nm, respectively.

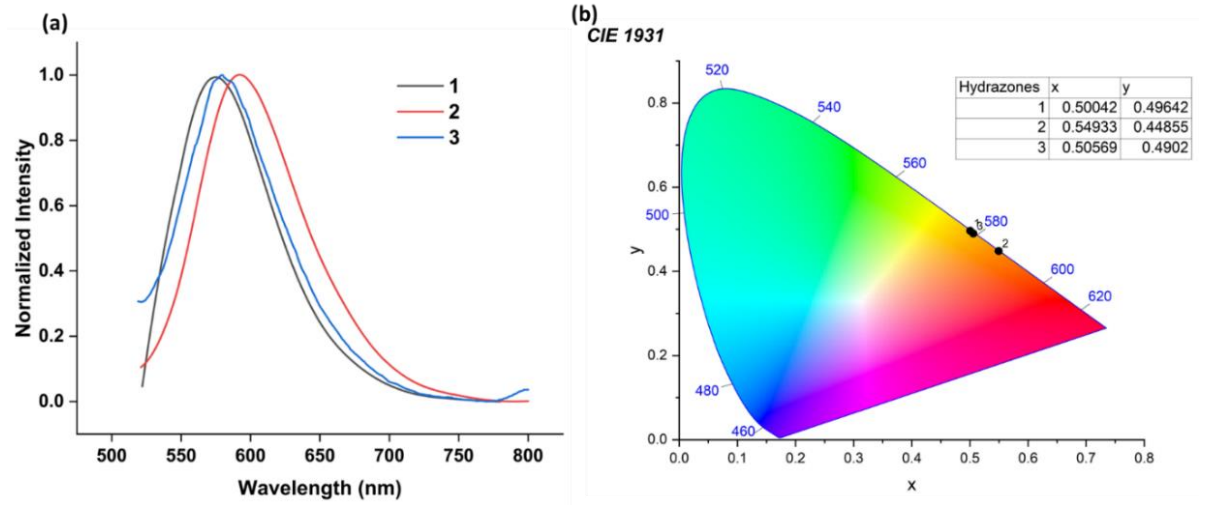

Figure S18. (a) Emission spectra (at 298 K) and (b) CIE chromaticity diagram of compounds **1**−**3** in isopropanol (c = 10^{-6} M). Compounds **1**−**3** are excited at λ_{ex} = 496 nm, λ_{ex} = 495 nm and λ_{ex} = 492 nm, respectively.

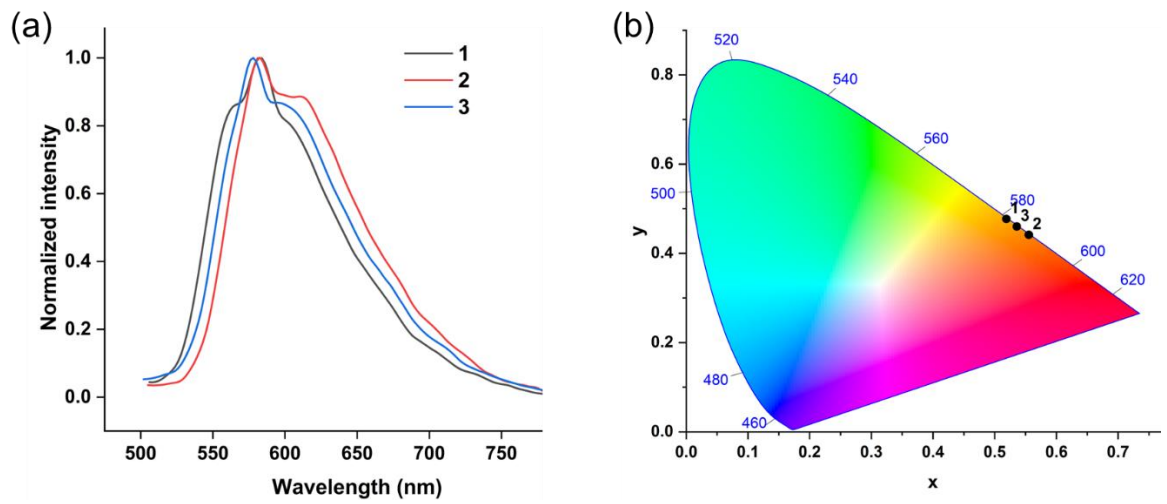

Figure S19. (a) Emission spectra (at 298 K) and (b) CIE chromaticity diagram of compounds **1**−**3** in toluene (c = 10^{-6} M). Compounds **1**−**3** are excited at λ_{ex} = 496 nm, λ_{ex} = 495 nm and λ_{ex} = 492 nm, respectively.

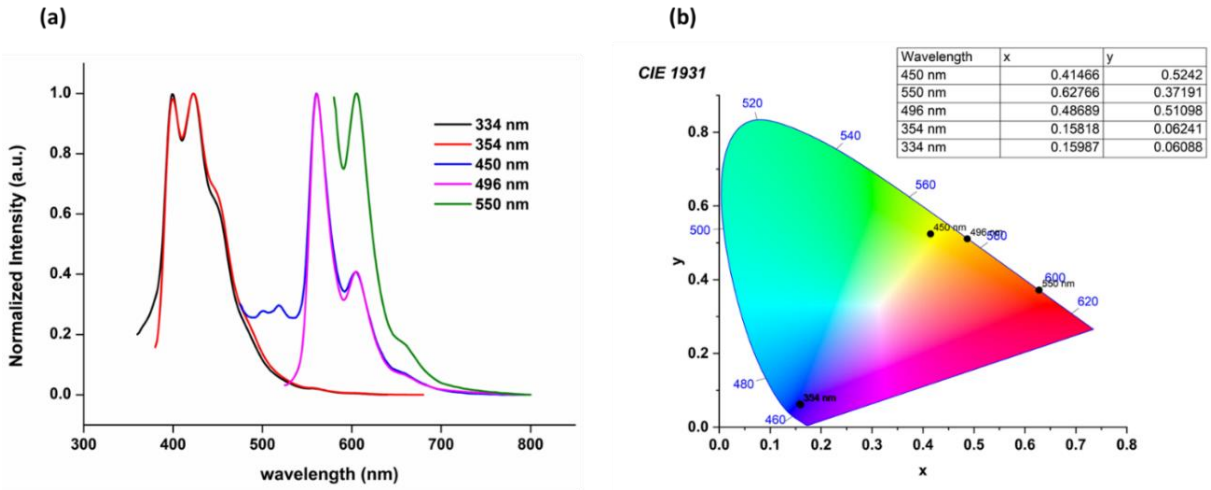

Figure S20. (a) Emission spectra (at 298 K) and (b) CIE chromaticity diagram of compound **1** in acetonitrile with different excited wavelengths (c = 10^{-6} M).

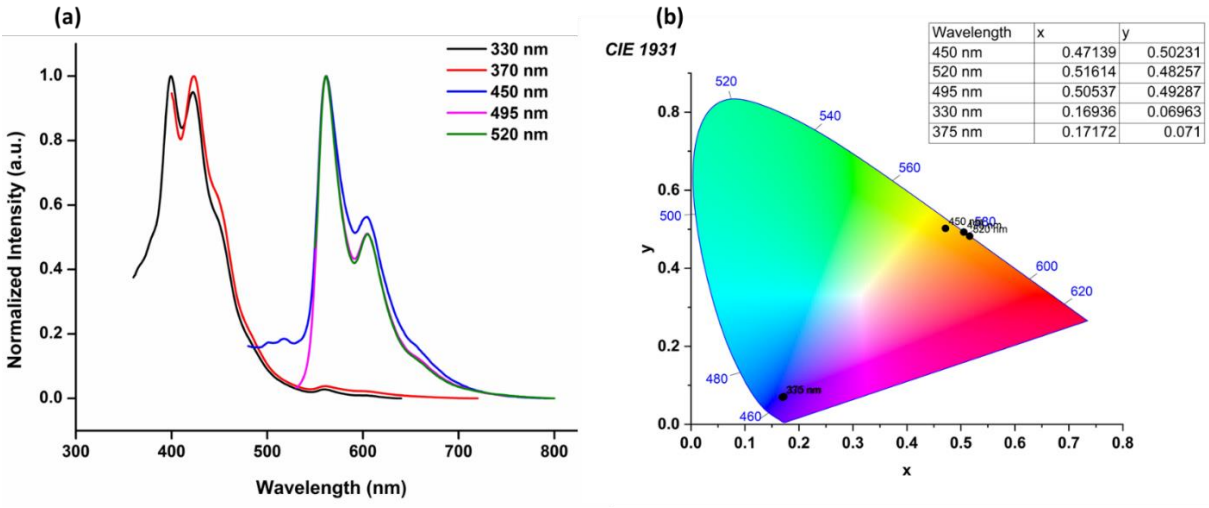

Figure S21. (a) Emission spectra (at 298 K) and (b) CIE chromaticity diagram of compound **2** in acetonitrile with different excited wavelengths (c = 10^{-6} M).

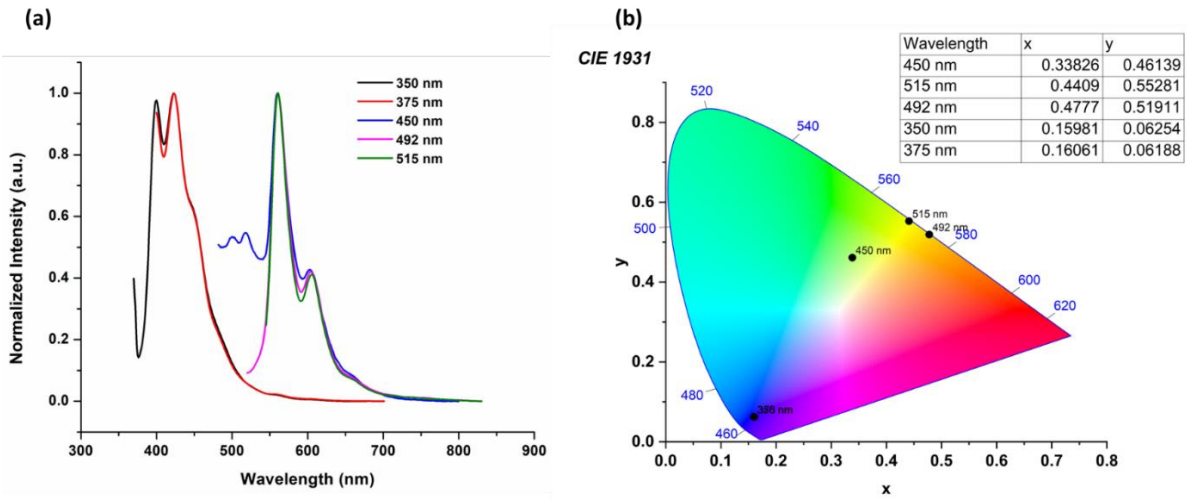

Figure S22. (a) Emission spectra (at 298 K) and (b) CIE chromaticity diagram of compound **3** in acetonitrile with different excited wavelengths (c = 10^{-6} M).

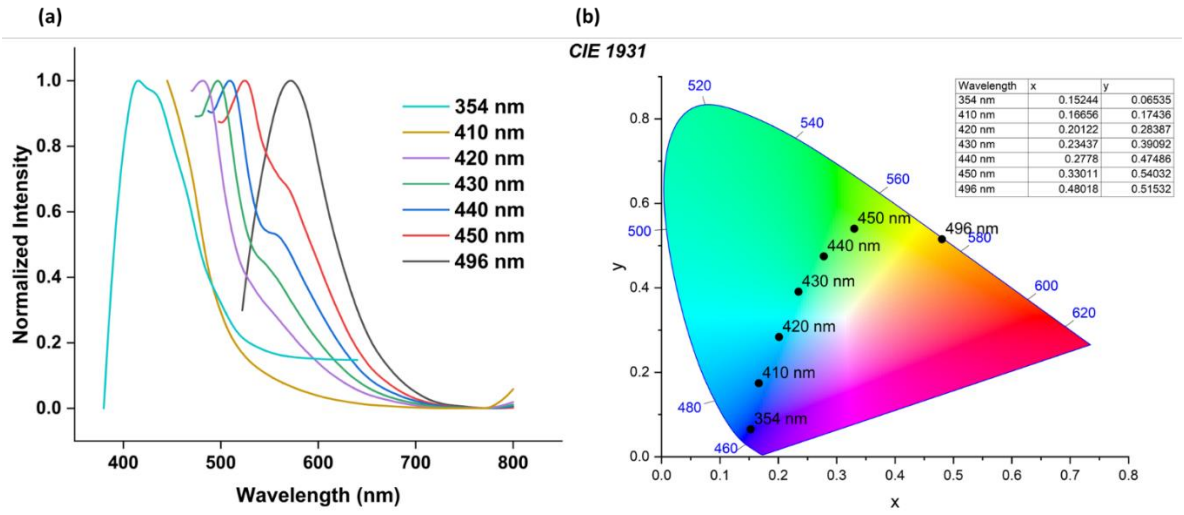

Figure S23. (a) Emission spectra (at 298 K) and (b) CIE chromaticity diagram of compound **1** in DMF with different excited wavelengths (c = 10^{-6} M).

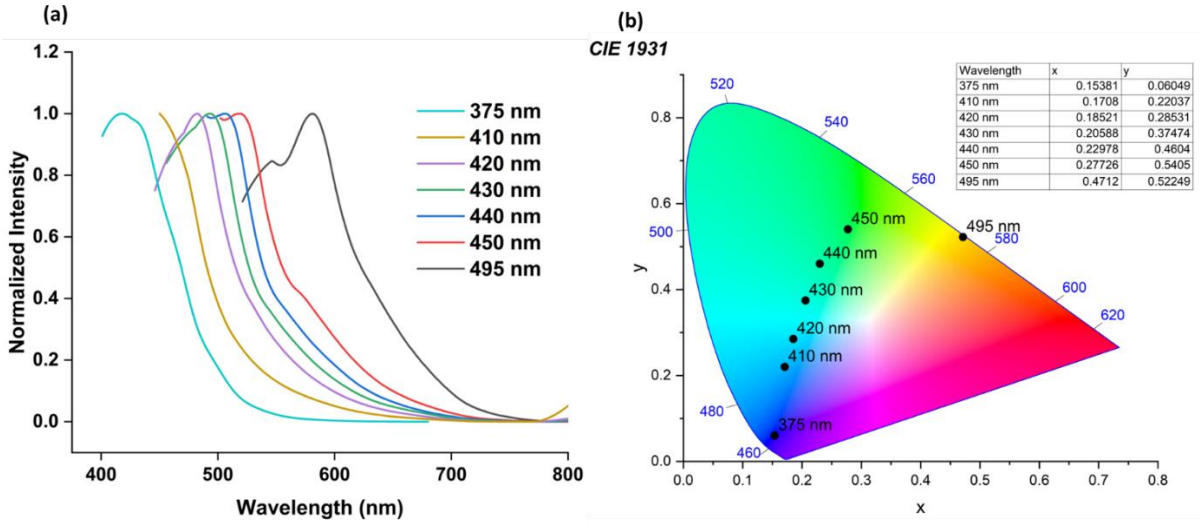

Figure S24. (a) Emission spectra (at 298 K) and (b) CIE chromaticity diagram of compound **2** in DMF with different excited wavelengths (c = 10^{-6} M).

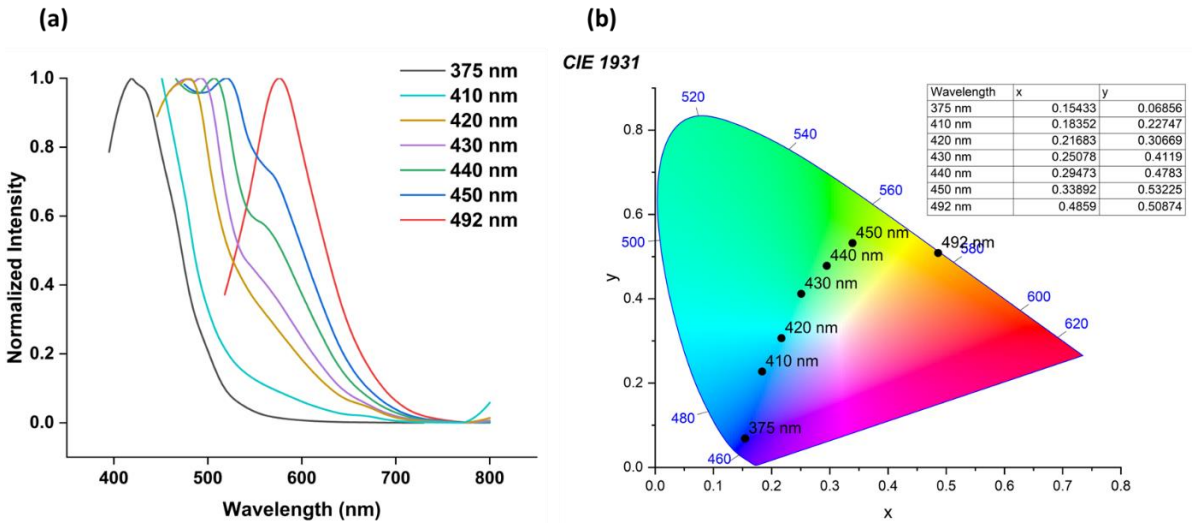

Figure S25. (a) Emission spectra (at 298 K) and (b) CIE chromaticity diagram of compound **3** in DMF with different excited wavelengths (c = 10^{-6} M).

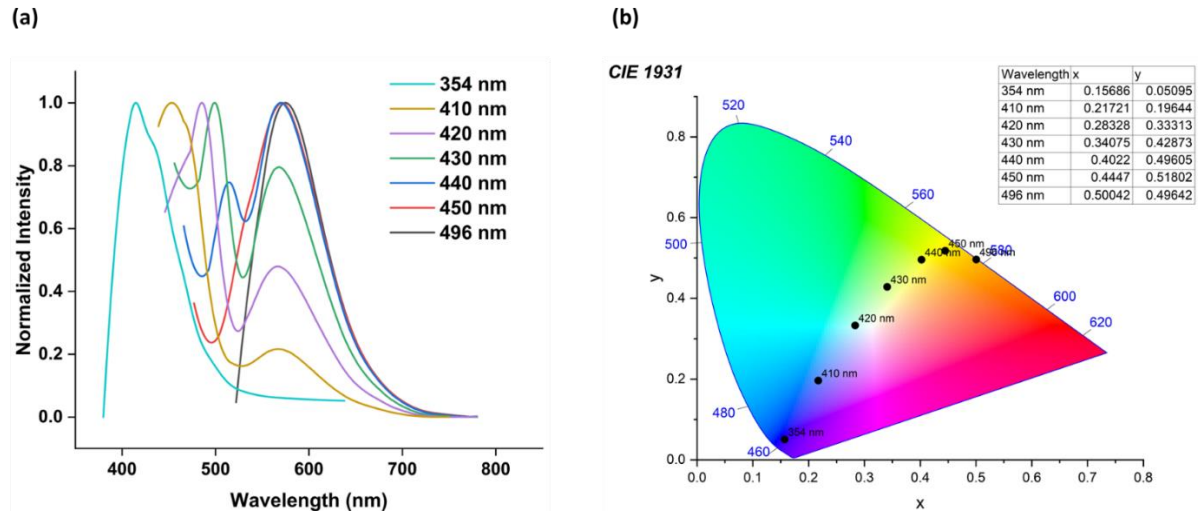

Figure S26. (a) Emission spectra (at 298 K) and (b) CIE chromaticity diagram of compound **1** in isopropanol with different excited wavelengths (c = 10^{-6} M).

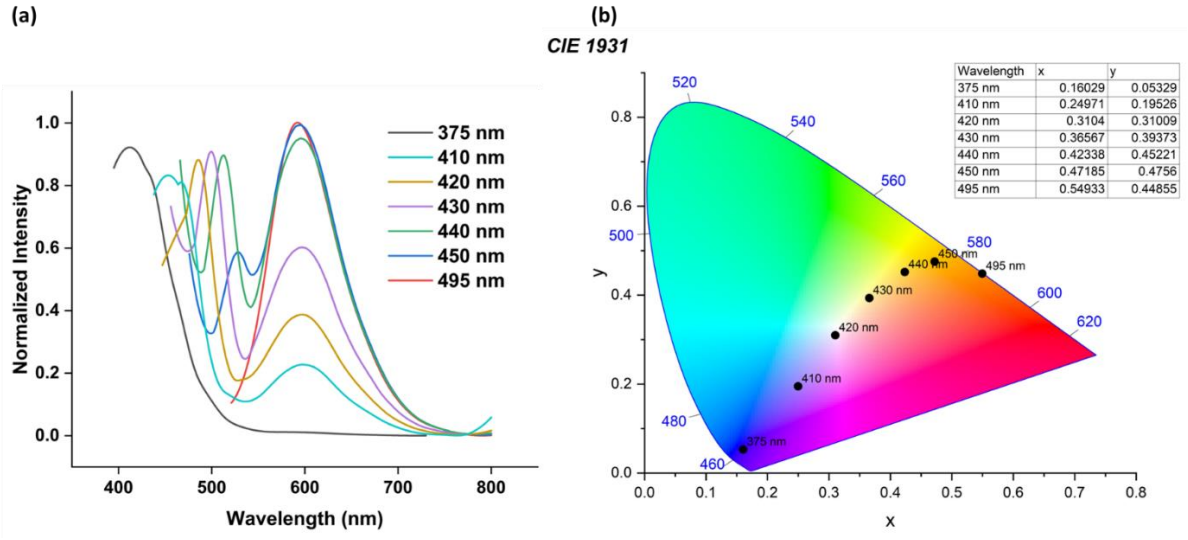

Figure S27. (a) Emission spectra (at 298 K) and (b) CIE chromaticity diagram of compound **2** in isopropanol with different excited wavelengths (c = 10^{-6} M).

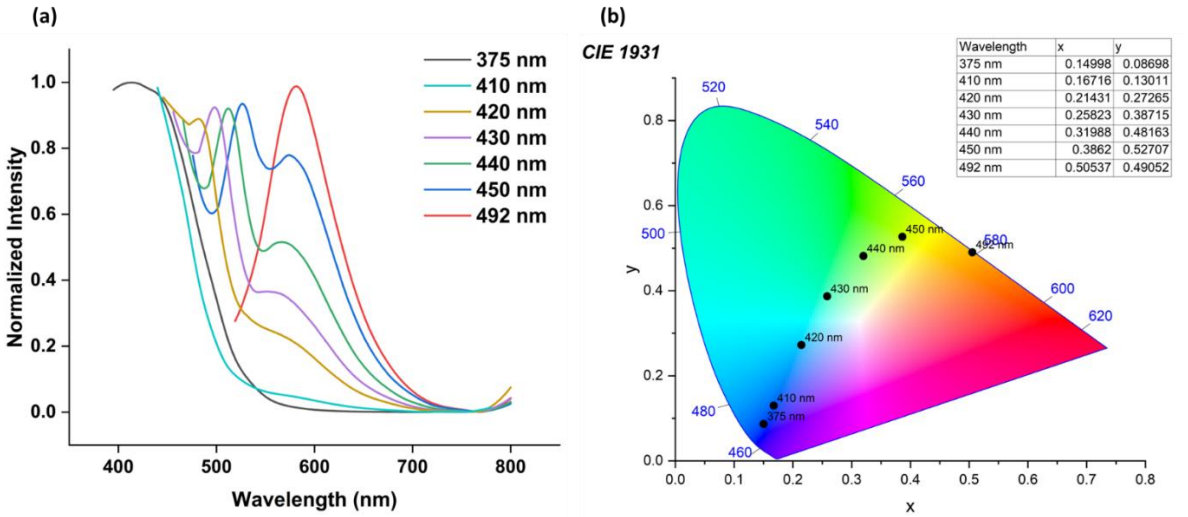

Figure S28. (a) Emission spectra (at 298 K) and (b) CIE chromaticity diagram of compound **3** in isopropanol with different excited wavelengths (c = 10^{-6} M).

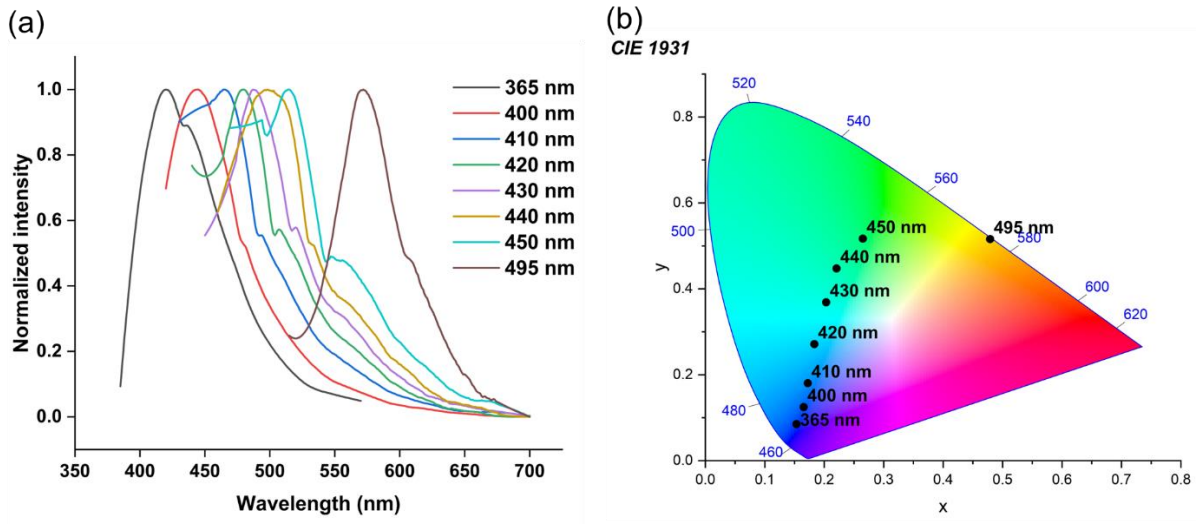

Figure S29. (a) Emission spectra (at 298 K) and (b) CIE chromaticity diagram of compound **1** in DMSO with different excited wavelengths (c = 10^{-6} M).

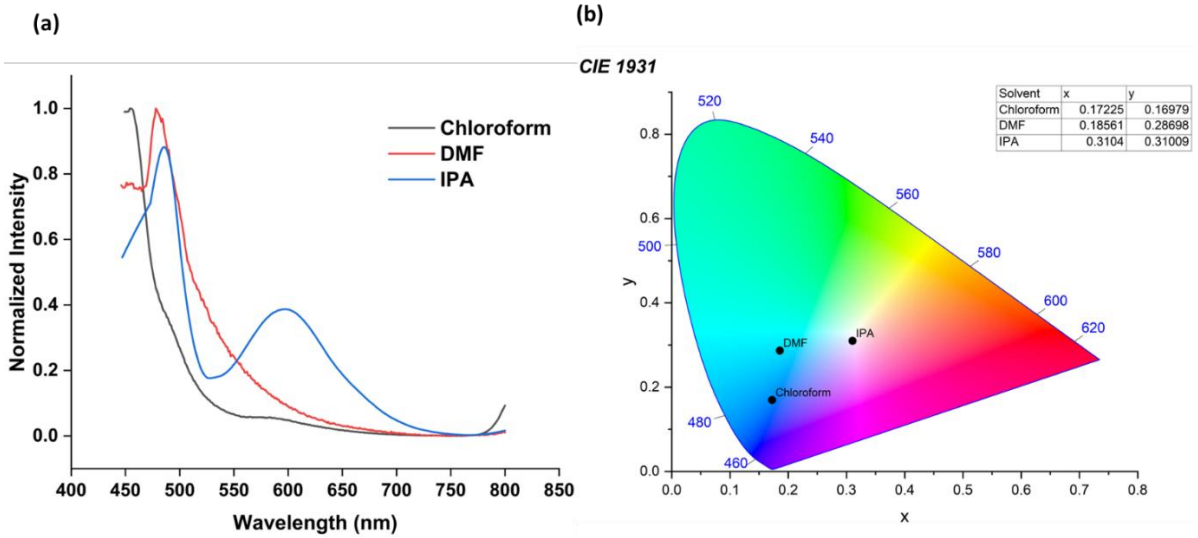

Figure S30. (a) Emission spectra (at 298 K) and (b) CIE chromaticity diagram of compound **2** in different solvents at λ_{ex} = 420 nm (c = 10^{-6} M).

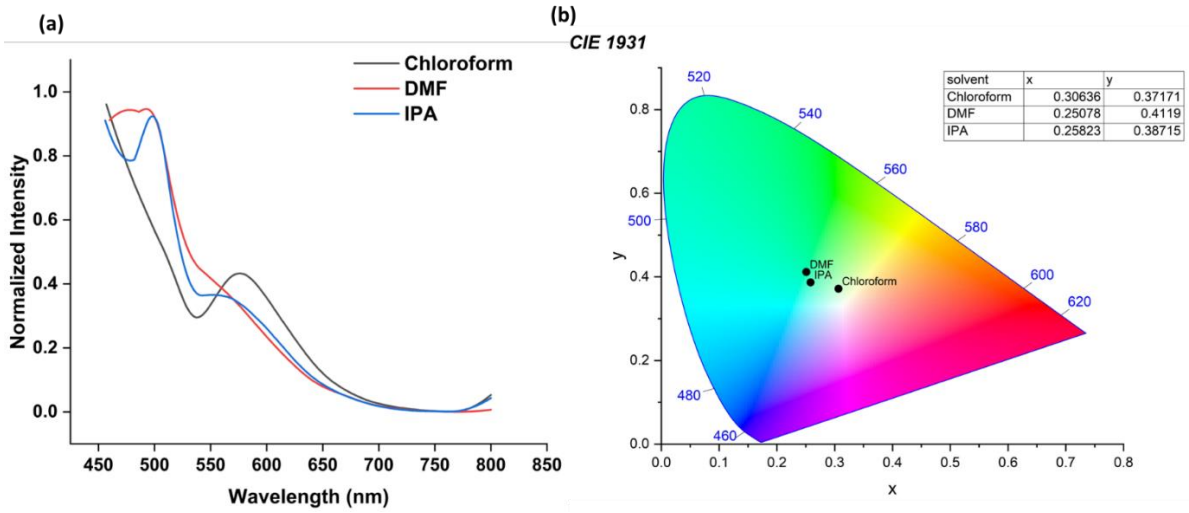

Figure S31. (a) Emission spectra (at 298 K) and (b) CIE chromaticity diagram of compound **3** in different solvents at λ_{ex} = 430 nm (c = 10^{-6} M).

6. Fluorescence spectrum of hydrazone 1−3 in solid state

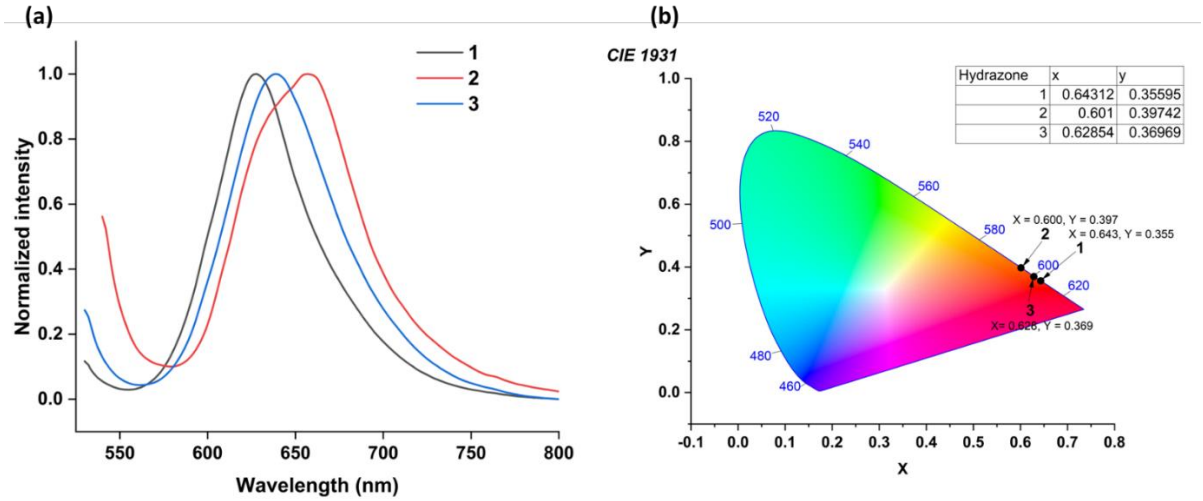

Figure S32. (a) Emission spectra (at 298 K) and (b) CIE chromaticity diagram of compounds **1−3** in solid-state. Compounds **1−3** are excited at λ_{ex} = 496 nm, λ_{ex} = 495 nm and λ_{ex} = 492 nm, respectively.

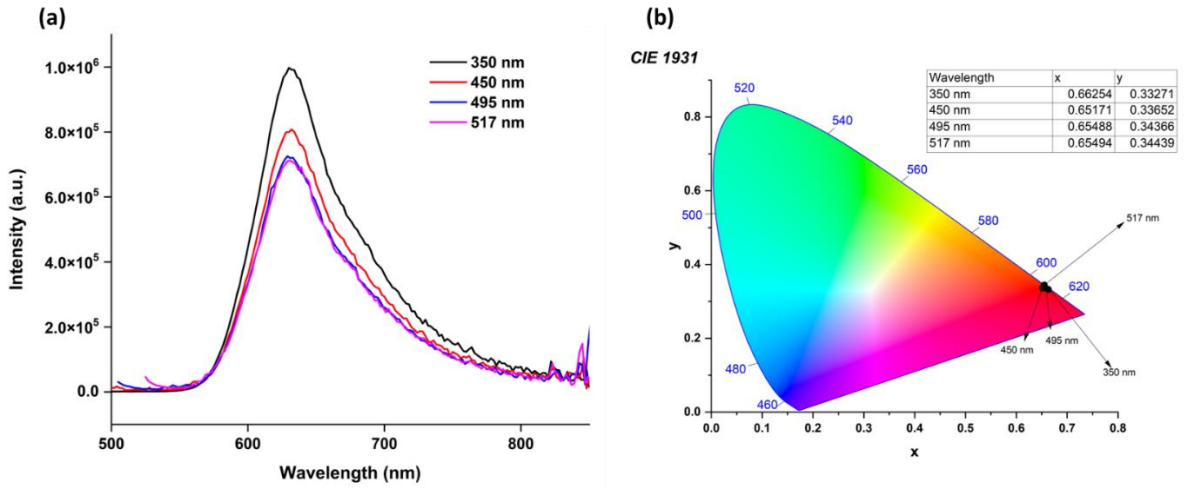

Figure S33. (a) Emission spectra (at 298 K) and (b) CIE chromaticity diagram of compound **1** in solid-state while excited with different wavelengths.

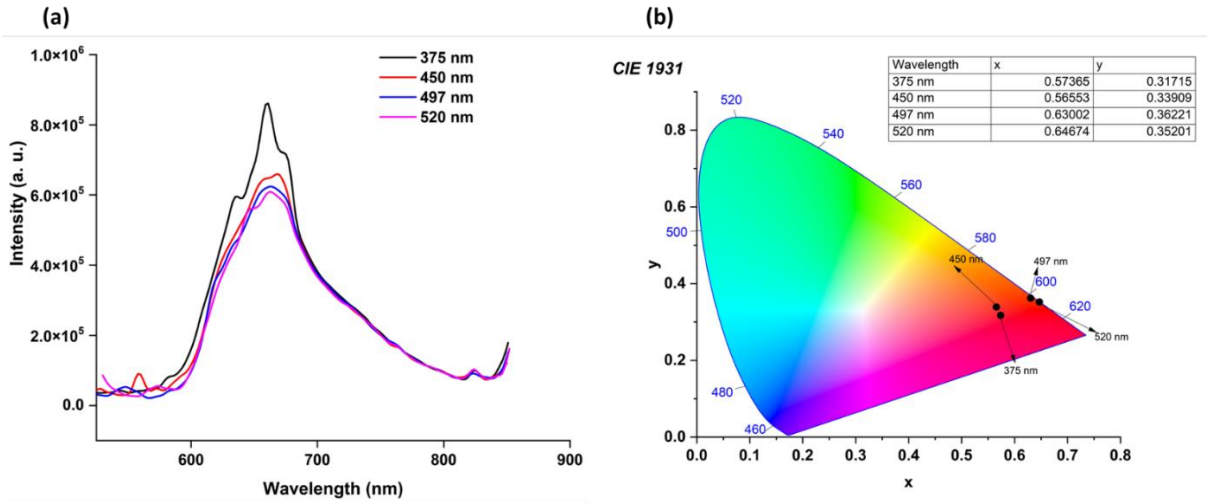

Figure S34. (a) Emission spectra (at 298 K) and (b) CIE chromaticity diagram of compound **2** in solid-state while excited with different wavelengths.

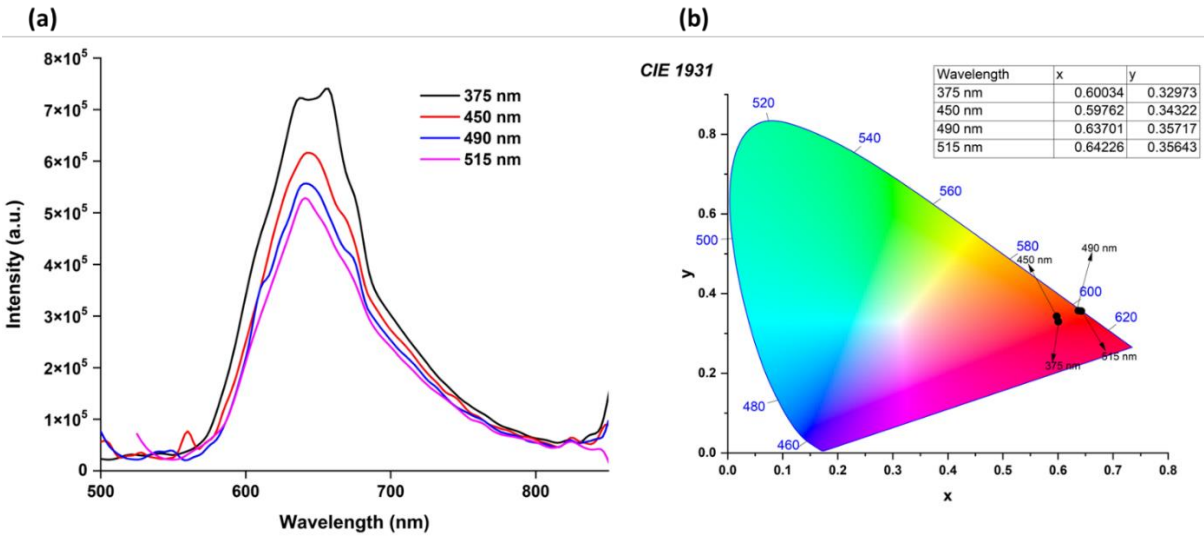

Figure S35. (a) Emission spectra and (b) CIE chromaticity diagram of compound **3** in solid state while excited with different wavelengths.

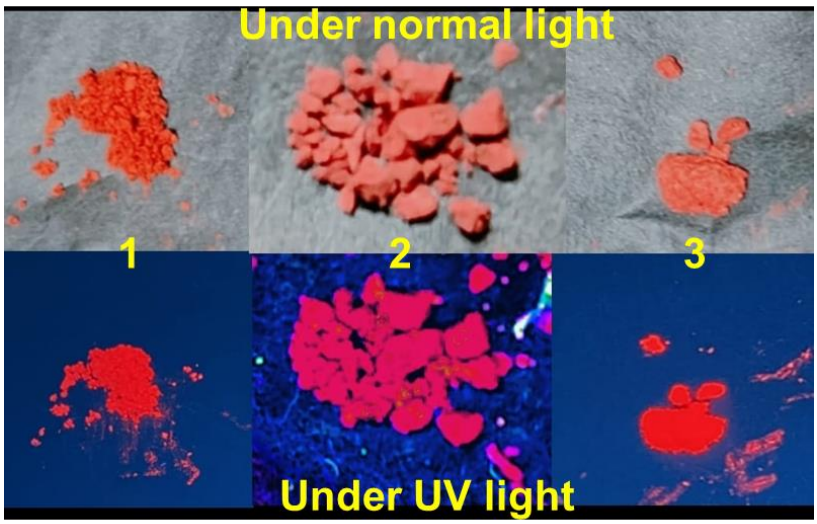

Figure S36. Digital photograph of the compounds (top) under normal light and (bottomed) under UV light.

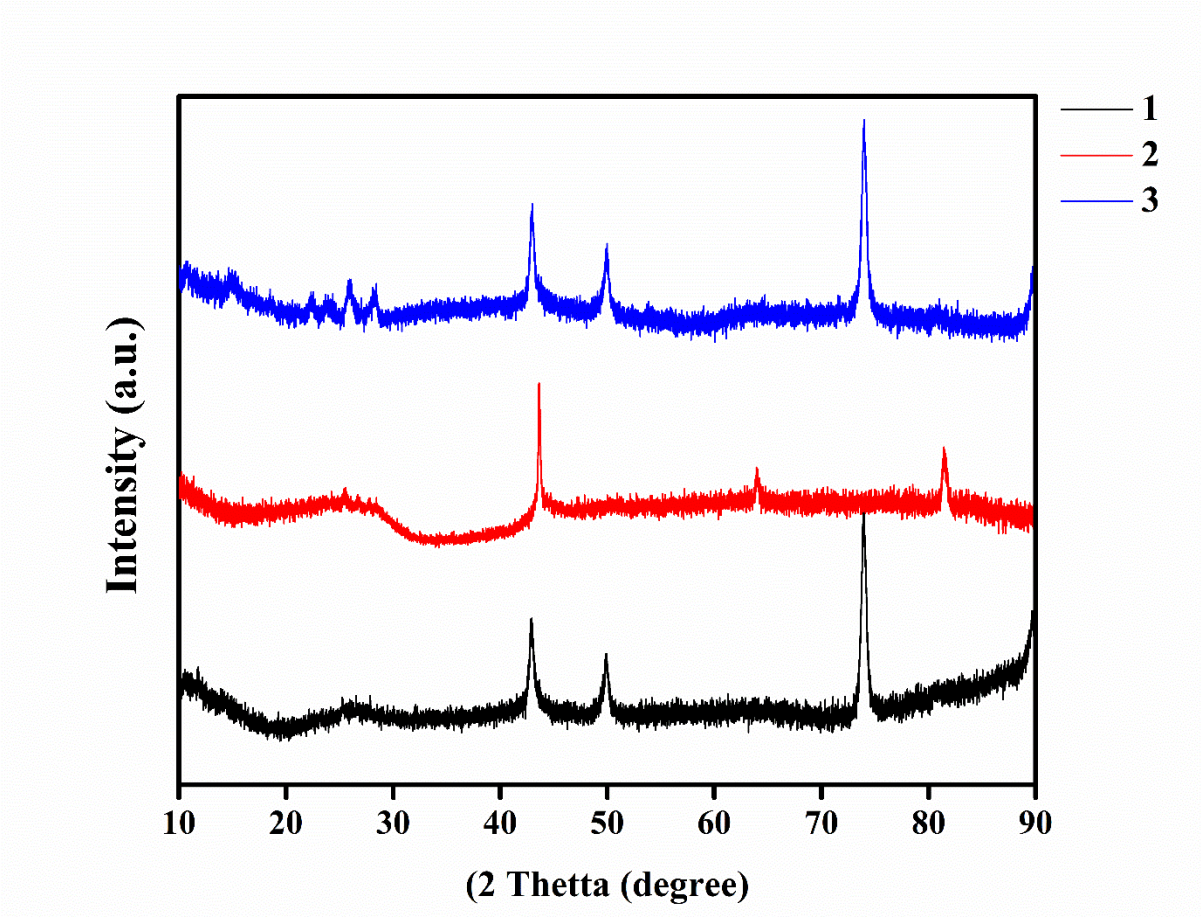

Figure S37. Powder XRD of hydrazones **1**–**3.**

7. Excitation spectra of hydrazone 1–3 in solution

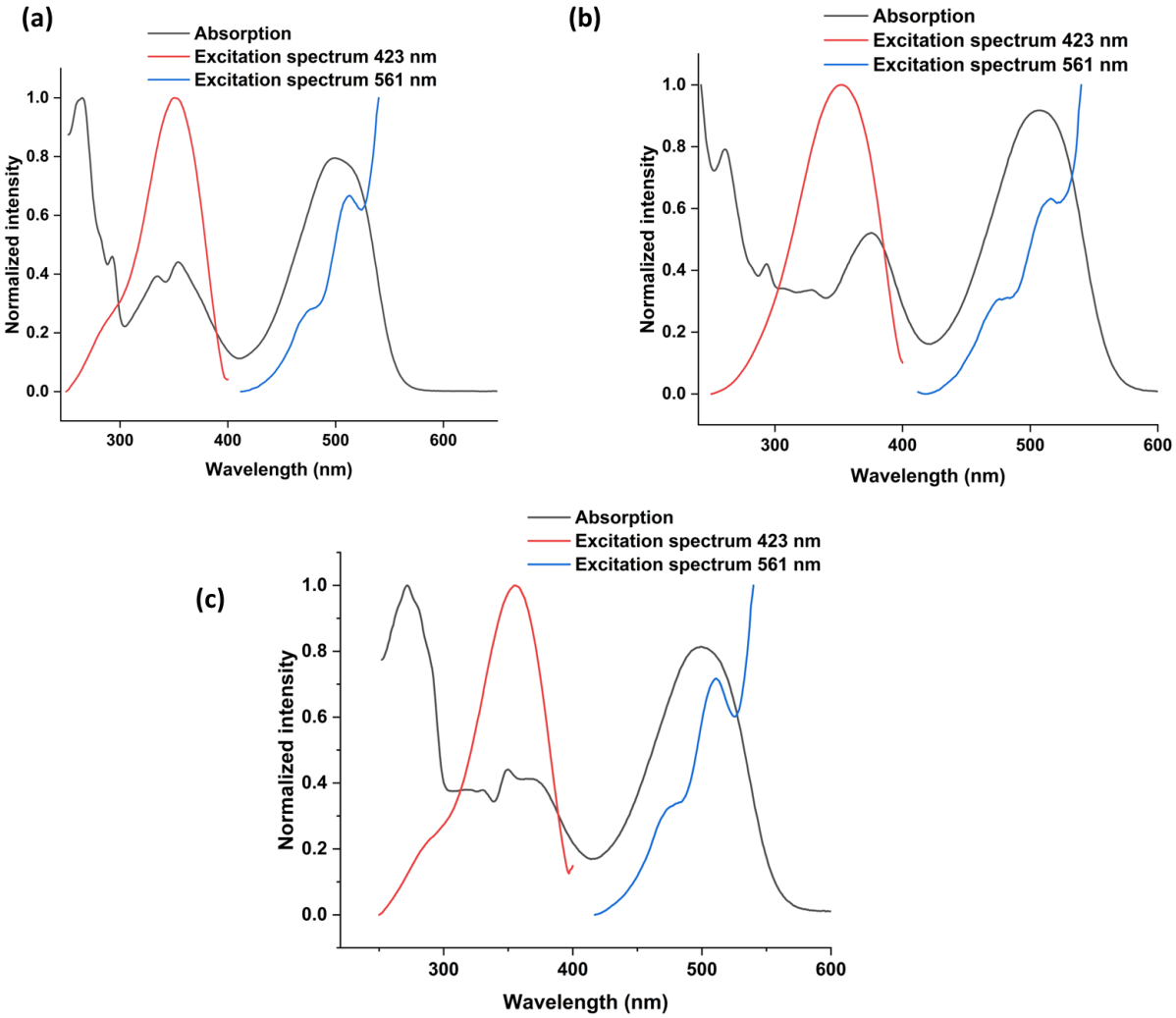

Figure S38. (a) Comparison of absorption and excitation spectra of (a) hydrazone **1** (at 298 K); (b) hydrazone **2** and (c) hydrazone **3** in acetonitrile (c = 10^{-5}M) for the emissions at 423 nm and 561 nm.

8. Fluorescence lifetime measurements

8.1 Fluorescence lifetime measurements in solution

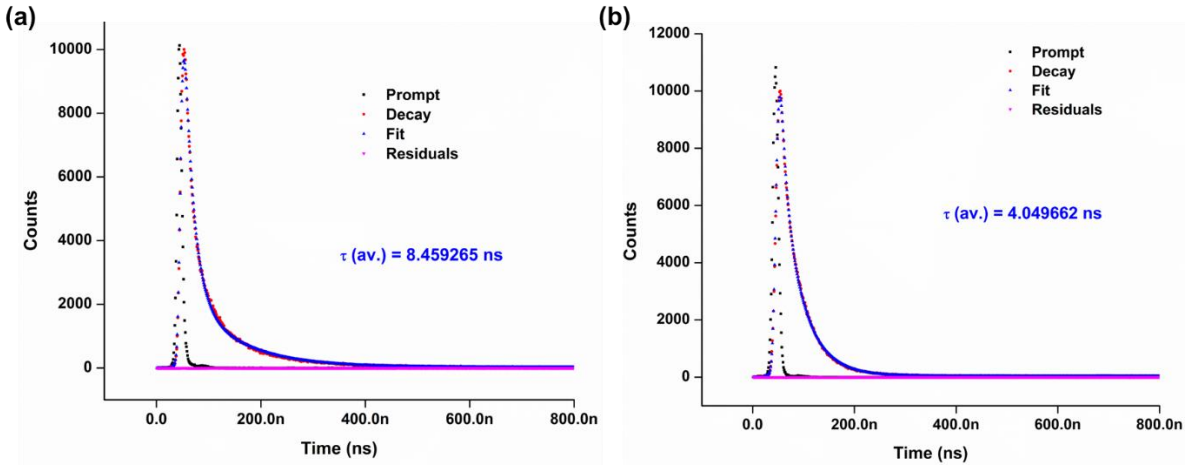

Figure S39. Fluorescence lifetime profile of compound **1** (a) λ_{ex} = 370 nm (b) λ_{ex} = 495 nm in acetonitrile at 298 K (c = 10^{-6} M).

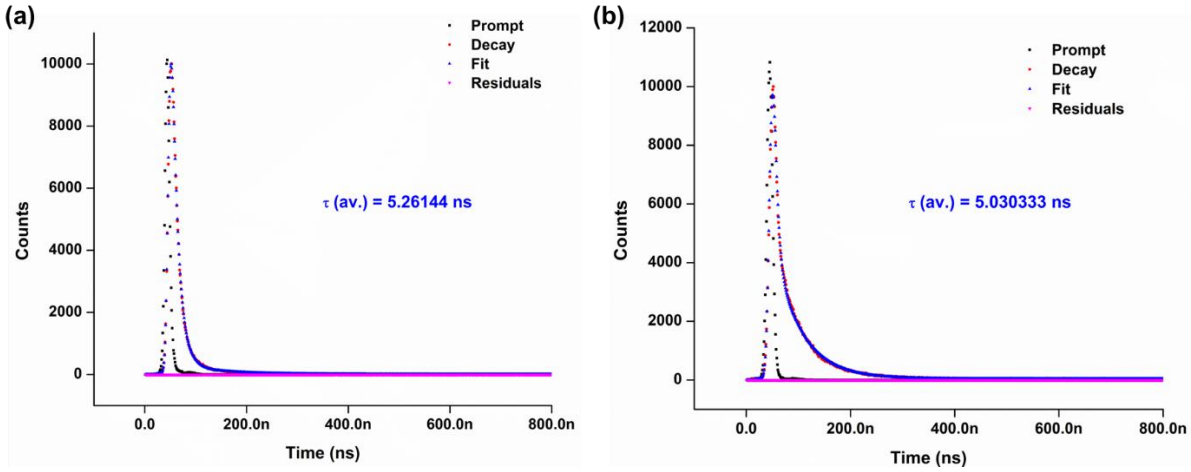

Figure S40. Fluorescence lifetime profile of compound **2** (a) λ_{ex} = 370 nm (b) λ_{ex} = 495 nm in acetonitrile at 298 K (c = 10^{-6} M).

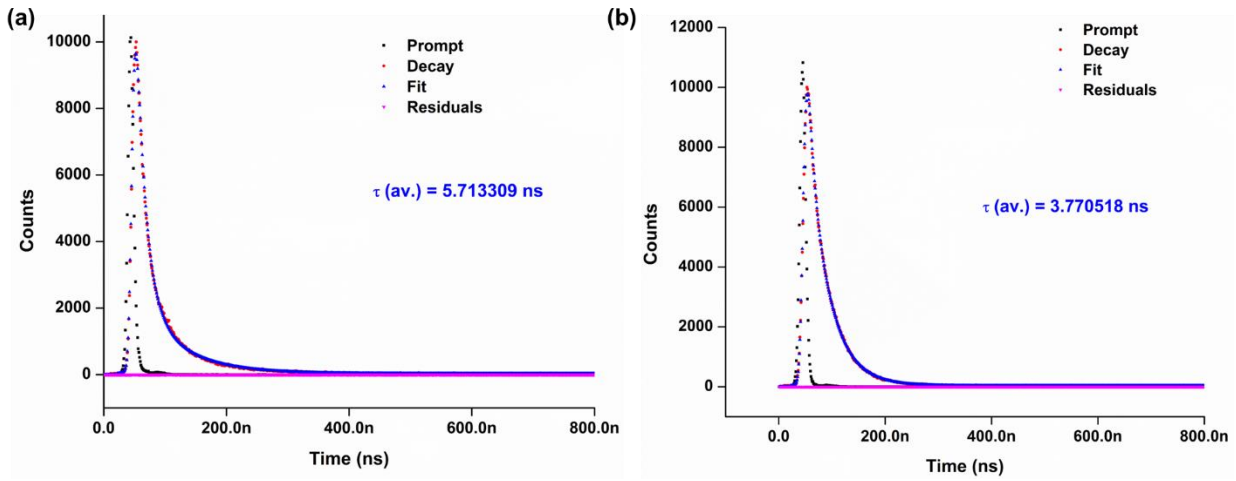

Figure S 41. Fluorescence lifetime profile of compound **3** (a) λ_{ex} = 370 nm (b) λ_{ex} = 495 nm in acetonitrile at 298 K (c = 10^{-6} M).

8.2 Fluorescence lifetime of hydrazone 1–3 in solid state

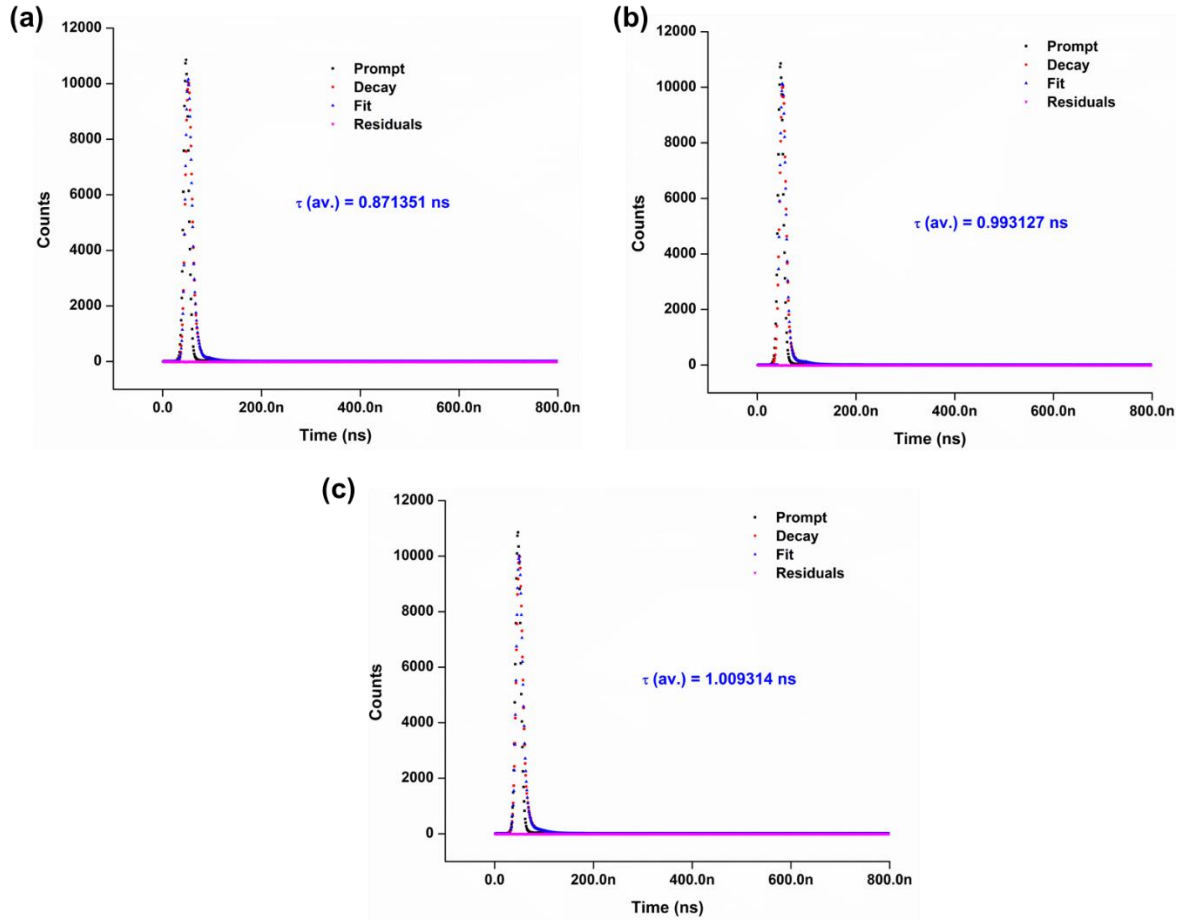

Figure S42. Fluorescence lifetime profile of (a) compound **1**; (b) compound **2** and (c) compound **3** in solid state (λ_{ex} = 495 nm).

9. Quantum Yields Measurement

The quantum yields of all compounds were determined using $[Ru(bpy)_3](PF_6)_2$ as a reference with a known $\Phi_R = 0.062$. According to the following equation, the quantum yield is calculated:

$$\Phi_S = \Phi_R \times \frac{1 - 10^{-A_R}}{1 - 10^{-A_S}} \times \frac{I_S}{I_R} \times \frac{{\eta_S}^2}{{\eta_R}^2}$$

Where Φ_S and Φ_R are the quantum yields of the sample and reference, respectively. A_S and A_R are the absorbance at the excitation wavelength of sample and reference, respectively. The area under the emission spectra of the sample and the reference are denoted as I_S and I_R respectively. The η_S and η_R are the refractive index of the respective solvents used in this study at 25°C (here, acetonitrile).

The absolute quantum yields in the solid-states were measured using the integrated sphere method employing Xenon lamp.

Table S1. Summary of photophysical studies performed in solutions and solid state.

Hydrazone	Solution[a]											Solid		
	acetonitrile							DMF						
	$\lambda_{abs.}$ (nm)	λ_{em} (nm)[b]	τ_{FL} (ns)	Φ_{FL} (%)	λ_{em} (nm)[c]	τ_{FL} (ns)	Φ_{FL} (%)	λ_{em} (nm)[e]	Φ_{FL} (%)	λ_{em} (nm)[f]	Φ_{FL} (%)	λ_{em} (nm)	τ_{FL} (ns)	Φ_{FL} (%)[g]
1	499	423	5.71	0.03	561	3.77	0.001	415	0.006	572	0.002	628	1.00	29
2	508	423	5.26	_[d]	563	5.03	_[d]	418	0.03	581	0.005	657	0.99	2
3	499	423	8.48	0.06	561	4.05	0.001	419	0.005	576	0.002	639	0.87	17

[a] Absorption and quantum yields were measured at $c = 10^{-5}$ M, and PL and lifetimes data were collected at $c = 10^{-6}$ M. [b] λ_{ex} < 365 nm. [c] λ_{ex} = 495 nm. [d] Too low to be measured. [e] λ_{ex} = 350 nm. [f] λ_{ex} = 500 nm. [g] The quantum yields were measured using the thin films.

10. DFT Calculations

The geometry optimizations and time-dependent density functional (TD-DFT) calculations of compounds **1-3** and pyrenedione (**5**) were carried out using DFT method with the Gaussian 16 using M062x function and Def2tzvp basis set. The molecular orbitals of excited states (**S_1-S_5**) were calculated using the same function and basis set and summarised in Figure S38. The electronic transitions to different excited states are listed in Table S2-S5.

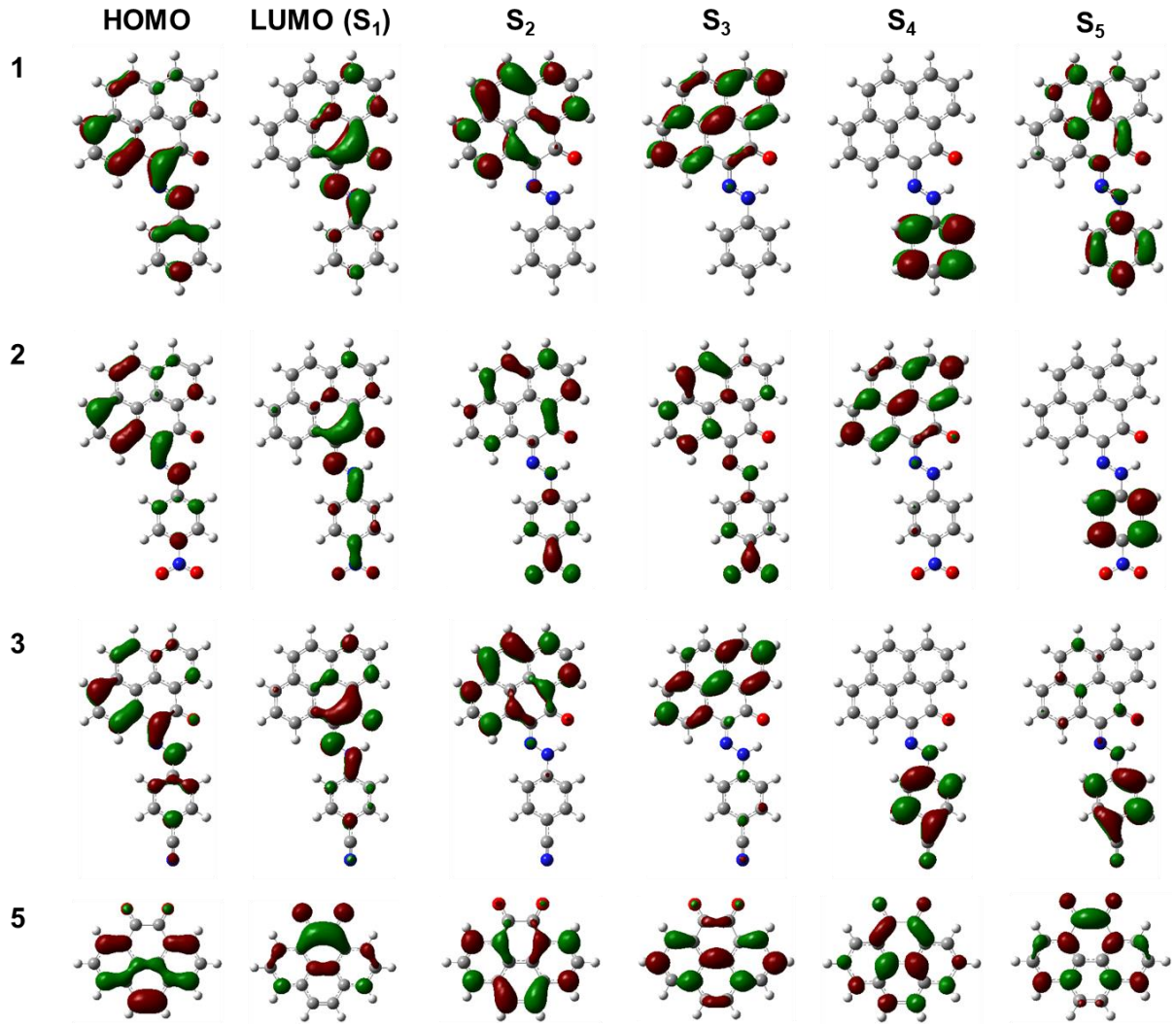

Figure S43. Molecular orbitals of the hydrazones **1-3** and **5**, **ES** represents excited state.

Table S2. Vertical excitations (ΔE in eV), oscillation strengths (*f*), orbital composition and transition dipole moments (μ in a.u.) and dipole square (μ^2) of low-lying states of Compound **5** (H_0, H_1, H_2, H_3 and H_4 represent HOMO, HOMO-1, HOMO-2, HOMO-3 and HOMO-4 orbitals, respectively. L_0, L_1, L_2 and L_6 are corresponding to LUMO, LUMO+1, LUMO+2, LUMO+6 orbitals, respectively).

Excited state	Δ*E*(eV)	*f*	composition	μ (X, Y, Z)	μ^2
S_1	2.4146	0.0000	$H_2 \rightarrow L_0$ $H_2 \rightarrow L_4$	-0.0000, -0.0000, -0.0090	0.0001
S_2	3.5886	0.0400	$H_0 \rightarrow L_0$	0.0004, 0.7003, -0.0001	0.4905
S_3	3.6595	0.0206	$H_1 \rightarrow L_0$	-0.4789, -0.0003, -0.0000	0.2294
S_4	3.7357	0.0000	$H_5 \rightarrow L_0$ $H_5 \rightarrow L_4$ $H_2 \rightarrow L_1$	-0.0001, -0.0000, -0.0000	0.0000
S_5	4.5937	0.0594	$H_1 \rightarrow L_1$ $H_0 \rightarrow L_0$	0.0000, 0.7268, -0.0001	0.5282
S_6	4.6539	0.1591	$H_1 \rightarrow L_2$ $H_0 \rightarrow L_1$	1.1812, -0.0003, 0.0000	1.3952

Table S3. Vertical excitations (ΔE in eV), oscillation strengths (*f*), orbital composition and transition dipole moments (μ in a.u.) and dipole square (μ^2) of low-lying states of Compound **1** (H_0, H_1, H_2, H_3 and H_4 represent HOMO, HOMO-1, HOMO-2, HOMO-3 and HOMO-4 orbitals, respectively. L_0, L_1, L_2 and L_6 are corresponding to LUMO, LUMO+1, LUMO+2, LUMO+6 orbitals, respectively).

Excited state	Δ*E*(eV)	*f*	composition	μ (X, Y, Z)	μ^2
S_1	3.0686	0.5723	$H_0 \rightarrow L_0$	-2.7486, 0.2400, 0.0002	7.6124
S_2	3.1804	0.0003	$H_4 \rightarrow L_0$ $H_4 \rightarrow L_6$	-0.0050, 0.0004, -0.0577	0.0034
S_3	3.8641	0.0001	$H_1 \rightarrow L_0$ $H_0 \rightarrow L_1$	-0.0203, -0.0231, 0.0000	0.0009
S_4	4.0186	0.1774	$H_2 \rightarrow L_0$ $H_1 \rightarrow L_1$ $H_0 \rightarrow L_1$	-1.2548, -0.4766, 0.0001	1.8018
S_5	4.2705	0.1196	$H_1 \rightarrow L_2$ $H_0 \rightarrow L_1$	-0.0109, -1.0692, -0.0001	1.1434
S_6	4.4268	0.0661	$H_2 \rightarrow L_0$ $H_2 \rightarrow L_1$ $H_0 \rightarrow L_1$ $H_0 \rightarrow L_2$	-0.3518, -0.6970, 0.0001	0.6096

Table S4. Vertical excitations (ΔE in eV), oscillation strengths (*f*), orbital composition and transition dipole moments (μ in a.u.) and dipole square (μ^2) of low-lying states of Compound **2** (H_0, H_1, H_2 and H_3 represent HOMO, HOMO-1, HOMO-2, HOMO-3 orbitals, respectively. L_0, L_1, L_2 and L_3 are corresponding to LUMO, LUMO+1, LUMO+2, LUMO+3 orbitals, respectively).

Excited state	Δ*E*(eV)	*f*	composition	μ (X, Y, Z)	μ^2
S_1	3.0111	0.6698	$H_0 \rightarrow L_0$	-3.0110, 0.1128, -0.0002	9.0788
S_2	3.1339	0.0002	$H_3 \rightarrow L_0$ $H_3 \rightarrow L_1$	0.0074, -0.0003, -0.0537	0.0029
S_3	3.7158	0.0044	$H_1 \rightarrow L_0$ $H_1 \rightarrow L_2$	0.0657, 0.2088, -0.0000	0.0479
S_4	3.9455	0.2818	$H_2 \rightarrow L_0$ $H_2 \rightarrow L_1$ $H_1 \rightarrow L_2$	-1.6565, -0.4132, 0.0000	2.9148
S_5	4.3111	0.0887	$H_2 \rightarrow L_0$ $H_2 \rightarrow L_2$ $H_1 \rightarrow L_0$ $H_1 \rightarrow L_1$ $H_1 \rightarrow L_3$ $H_0 \rightarrow L_1$	0.1072, 0.9101, -0.0001	0.8398
S_6	4.4572	0.0858	$H_2 \rightarrow L_0$ $H_1 \rightarrow L_1$ $H_0 \rightarrow L_2$ $H_0 \rightarrow L_3$	-0.1413, -0.8750, 0.0001	0.7856

Table S5. Vertical excitations (*ΔE* in eV), oscillation strengths (*f*), orbital composition and transition dipole moments (μ in a.u.) and dipole square (μ^2) of low-lying states of Compound **3** (H_0, H_1, H_2 and H_3 represent HOMO, HOMO-1, HOMO-2, HOMO-3 orbitals, respectively. L_0, L_1, L_2 and L_6 are corresponding to LUMO, LUMO+1, LUMO+2, LUMO+6 orbitals, respectively).

Excited state	Δ*E*(eV)	*f*	composition	μ (X, Y, Z)	μ^2
S_1	3.0267	0.6616	$H_0 \rightarrow L_0$	2.9834, 0.1481, 0.0001	8.9226
S_2	3.1447	0.0001	$H_4 \rightarrow L_0$ $H_4 \rightarrow L_6$	-0.0020, -0.0001, 0.0431	0.0019
S_3	3.7459	0.0035	$H_1 \rightarrow L_0$ $H_0 \rightarrow L_1$	-0.0624, 0.1842, 0.0000	0.0378
S_4	3.9575	0.2484	$H_2 \rightarrow L_0$ $H_1 \rightarrow L_1$ $H_1 \rightarrow L_0$ $H_0 \rightarrow L_2$	1.5496, -0.4005, 0.0000	2.5617
S_5	4.3093	0.1014	$H_1 \rightarrow L_1$ $H_1 \rightarrow L_2$ $H_0 \rightarrow L_1$	0.0162, -0.9798, -0.0000	0.9604
S_6	4.4508	0.0847	$H_2 \rightarrow L_0$ $H_2 \rightarrow L_1$ $H_0 \rightarrow L_1$ $H_0 \rightarrow L_2$	0.1295, -0.8719, 0.0000	0.7770

Ground state Optimized coordinates

Compound **1**

C	3.57184500	-3.09412200	-0.00009100
C	2.19713000	-2.87217600	-0.00009600
C	1.69790500	-1.58134000	-0.00004800
C	2.57037500	-0.47372000	-0.00000400
C	3.96390400	-0.70405700	-0.00000100
C	4.44004000	-2.02270800	-0.00004200
H	3.95669200	-4.10521600	-0.00012500
H	1.49507000	-3.69520800	-0.00013100
H	5.51101100	-2.18833600	-0.00003900
C	2.06800100	0.87366000	0.00002500
C	2.98062100	1.95166600	0.00006300
C	0.67822600	1.12787100	0.00001000
C	2.49523200	3.26554300	0.00009000
C	0.23464500	2.44146600	0.00003600
C	1.13826700	3.50170100	0.00007700

H	3.19972000	4.08813200	0.00012000
H	-0.82852800	2.63520100	0.00002200
H	0.76560200	4.51784400	0.00009700
C	-0.26287800	-0.00171400	-0.00002500
C	0.23475500	-1.38281700	-0.00005000
O	-0.53122200	-2.34660200	-0.00019400
N	-1.53776500	0.29200500	0.00000000
N	-2.45235000	-0.62625700	0.00012700
H	-2.15046500	-1.60237400	0.00031900
C	-3.81052800	-0.29153100	0.00005600
C	-4.73541400	-1.33284300	0.00021500
C	-4.24339000	1.03173600	-0.00015800
C	-6.09076800	-1.04912900	0.00015700
H	-4.38655300	-2.35851400	0.00038400
C	-5.60201300	1.29903400	-0.00021400
H	-3.51527400	1.82943000	-0.00027400
C	-6.53222700	0.26693400	-0.00005900
H	-6.80441400	-1.86250300	0.00028100
H	-5.93781600	2.32793100	-0.00038000
H	-7.59106000	0.48712600	-0.00010300
C	4.86060000	0.41614400	0.00004200
H	5.92614500	0.22109900	0.00004700
C	4.39047000	1.67971600	0.00007300
H	5.07166900	2.52208300	0.00010400

Compound **2**

C	4.64487500	-3.00729200	0.00017900
C	3.26290200	-2.83469400	0.00018000
C	2.71878400	-1.56229500	0.00008600
C	3.55017600	-0.42343200	0.00000100
C	4.95029200	-0.60361100	0.00000200

C	5.47311800	-1.90526700	0.00008900
H	5.06566200	-4.00381100	0.00024900
H	2.59155500	-3.68293400	0.00024900
H	6.54929300	-2.03235500	0.00008900
C	3.00006600	0.90577400	-0.00007000
C	3.87452800	2.01433200	-0.00014900
C	1.60308200	1.11423900	-0.00006000
C	3.34305300	3.31102100	-0.00022300
C	1.11336600	2.41019300	-0.00013400
C	1.97966900	3.50188000	-0.00021600
H	4.01904900	4.15715000	-0.00028400
H	0.04416200	2.56711800	-0.00012500
H	1.57257900	4.50452700	-0.00027300
C	0.69797200	-0.04715000	0.00001700
C	1.25105500	-1.41725300	0.00009200
O	0.51854700	-2.40299500	0.00029200
N	-0.57988500	0.19960600	-0.00003700
N	-1.46608900	-0.76031000	-0.00023200
H	-1.12855300	-1.72389700	-0.00052600
C	-2.82336100	-0.47264100	-0.00012100
C	-3.71654500	-1.54736500	-0.00037700
C	-3.30014900	0.84001300	0.00022300
C	-5.07647600	-1.31658500	-0.00028600
H	-3.33551200	-2.56072800	-0.00064800
C	-4.66096800	1.06967800	0.00031600
H	-2.59930000	1.66077400	0.00041200
C	-5.53145500	-0.00840600	0.00006000
H	-5.78706100	-2.12983600	-0.00047900
H	-5.05995000	2.07343000	0.00058100
C	5.80736900	0.54698000	-0.00008100
H	6.87900000	0.38956900	-0.00008200
C	5.29294500	1.79315100	-0.00015400

H	5.94372300	2.65907800	-0.00021600
N	-6.97639400	0.24221200	0.00016000
O	-7.34634800	1.39532500	0.00047300
O	-7.71268200	-0.71936100	-0.00006900

Compound **3**

C	-4.23336400	-3.02047000	-0.00001700
C	-2.85260700	-2.83883200	-0.00002200
C	-2.31667200	-1.56291300	-0.00001400
C	-3.15566200	-0.42963700	0.00000000
C	-4.55467800	-0.61901200	0.00000500
C	-5.06900400	-1.92388900	-0.00000300
H	-4.64765500	-4.01973100	-0.00002300
H	-2.17557100	-3.68255100	-0.00003500
H	-6.14432500	-2.05807100	0.00000100
C	-2.61425300	0.90314500	0.00000800
C	-3.49579500	2.00616500	0.00002400
C	-1.21850400	1.12008000	0.00000600
C	-2.97277600	3.30614900	0.00003700
C	-0.73722100	2.41934600	0.00002300
C	-1.61046100	3.50538300	0.00003700
H	-3.65406900	4.14802000	0.00004900
H	0.33095800	2.58311000	0.00002300
H	-1.20972600	4.51062300	0.00004900
C	-0.30674300	-0.03572400	-0.00000900
C	-0.84969300	-1.40790100	-0.00003000
O	-0.11082800	-2.38970200	-0.00003400
N	0.97073100	0.21914800	0.00000400
N	1.86195500	-0.73343400	0.00005700
H	1.53048900	-1.69940800	0.00013300
C	3.21950700	-0.43725700	0.00002500
C	4.11964500	-1.50419300	0.00009900

C	3.68921100	0.87656500	-0.00007700
C	5.47765100	-1.26248500	0.00007200
H	3.74603400	-2.52050300	0.00017900
C	5.04875000	1.11226800	-0.00010300
H	2.98393200	1.69382400	-0.00013300
C	5.95261600	0.04889200	-0.00002900
H	6.17843300	-2.08601600	0.00013000
H	5.42282800	2.12709700	-0.00018100
C	-5.41914500	0.52616000	0.00001900
H	-6.48975400	0.36181800	0.00002400
C	-4.91284100	1.77562300	0.00002800
H	-5.56926400	2.63730300	0.00004000
C	7.36299500	0.30355800	-0.00005700
N	8.49282500	0.50799500	-0.00007900

Table S6. TD-DFT calculation of hydrazones **1-3** in their keto- and enol-forms at b3lyp/6-31+g* level. For the compounds **1** and **3** the energy differences in enol form are higher compared their keto-form while **2** shows a reverse trend. Based on the data from compounds **1** and **3** the possible mechanism for the radiative relaxation is postulated. The assignment of tautomeric emissions is also based on experimental observations: excitation with high energy lights <450 nm resulted in emissions in the blue region along with a peak at 561 nm which was intensified when excitation wavelengths are beyond 450 nm. Excitation with 450 and 495 nm, where the enol-form absorbs significantly, a major contribution was observed from the same. However, excitation with 550 nm, where keto-form absorbs mostly, resulted in strong emission from the same. This indicates that excitation with high energy light can promote ESIPT resulting in the emission from enol-from. Because the energy differences between HOMO and LUMO are similar we assume that the emission in the blue region occurs from the higher exited states rather than the locally excited $\mathbf{S_1}$ state.

Hydrazone	Keto-form		Enol-form	
	LUMO→HOMO (eV)	λ_{em} (nm)	LUMO→HOMO (eV)	λ_{em} (nm)
1	2.2197	558	2.4743	501
2	2.3869	519	2.1706	571
3	2.1163	585	2.2915	541

11. Single crystal X-ray diffraction

Single crystals, suitable for X-ray diffraction analysis, were grown by slow evaporation of a concentrated solution of the compounds. Data were collected on a Bruker D8 quest diffractometer with MoKα (λ = 0.71073) radiation. Preliminary lattice parameters and orientation matrices were obtained from two sets of frames. Then full data were collected using the ω and ϕ scan method with a frame width of 0.5° (Mo). Data were processed with the SAINT+ program for reduction and cell refinement. Multiscan absorption corrections were applied by using the SADABS program for area detector. The structures were solved by SHELXT[3] and refined with SHELXL[4] using Olex2 program.[5] Similar 1,2 and 1,3 bond length (SADI), fixed bond length (DFIX), similar U_{ij} (SIMU), rigid body (RIGU) and isotropic U_{ij} (ISOR) restraints were applied. The CIF file is submitted into CCDC (2294513) and can be obtained through https://summary.ccdc.cam.ac.uk/structure-summary-form.

Table S7. Refinement parameters for **1**.

Identification code	**1**
CCDC	2294513
Empirical formula	$C_{22}H_{14}N_2O$
Formula weight	322.33
Temperature/K	273.15
Crystal system	monoclinic
Space group	$P2_1$
a/Å	14.9310(11)
b/Å	4.4906(3)
c/Å	23.0319(16)
α/°	90
β/°	90.011(4)
γ/°	90
Volume/Å^3	1544.27(19)
Z	4
ρ_{calc}g/cm^3	1.386
μ/mm^{-1}	0.086

$F(000)$	672.0
Crystal size/mm^3	0.2 × 0.07 × 0.04
Radiation	MoKα (λ = 0.71073)
2Θ range for data collection/°	4.468 to 51.352
Index ranges	-18 ≤ h ≤ 18, -5 ≤ k ≤ 5, -28 ≤ l ≤ 28
Reflections collected	19788
Independent reflections	5771 [R_{int} = 0.0951, R_{sigma} = 0.1072]
Data/restraints/parameters	5771/2450/797
Goodness-of-fit on F^2	1.460
Final R indexes [I>=2σ (I)]	R_1 = 0.1490, wR_2 = 0.3912
Final R indexes [all data]	R_1 = 0.1898, wR_2 = 0.4230
Largest diff. peak/hole / e Å^{-3}	0.48/-0.55

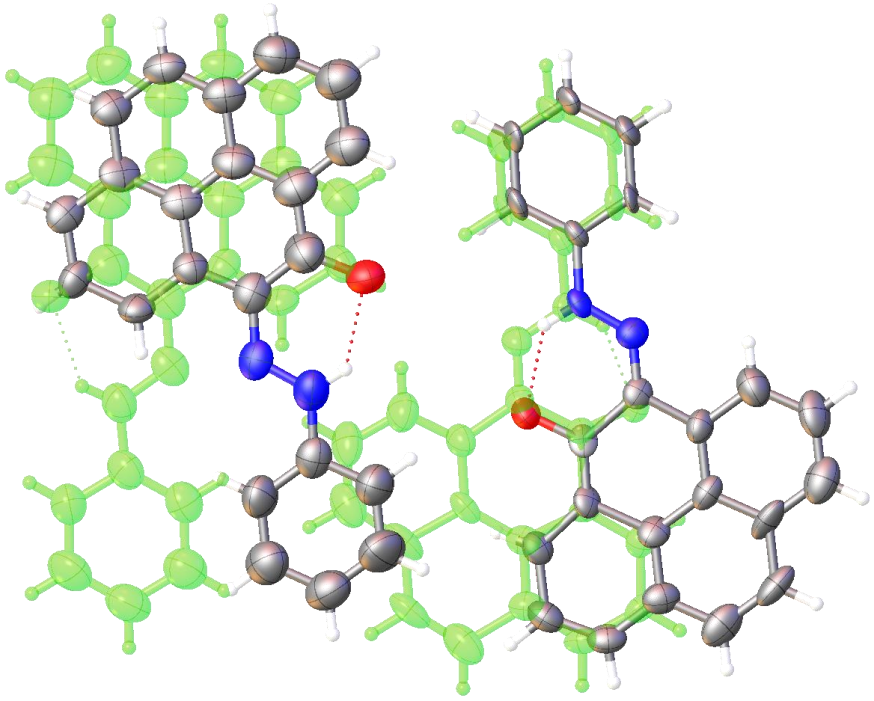

Figure S44. Asymmetric unit of **1** as determined by SCXRD analysis. The asymmetric unit contains two molecules disordered over two positions (~1:1 ratio). The disordered part is shown in green colour. Atoms are shown in thermal ellipsoids with 50% probability level.

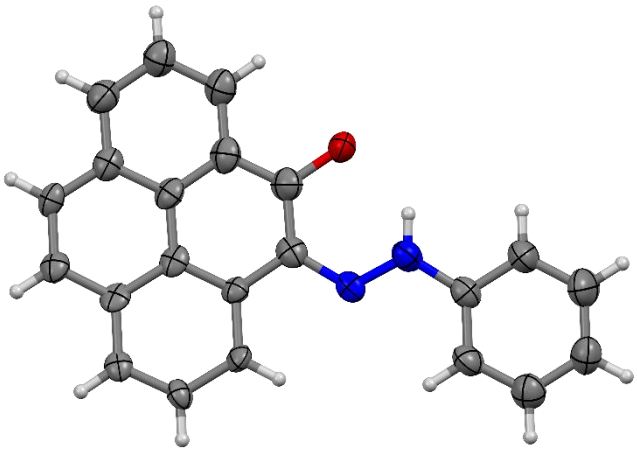

Figure S45. Molecular structure of **1** in thermal ellipsoid model. Disordered parts are removed for clarity. Atoms are shown in thermal ellipsoids with 50% probability level.

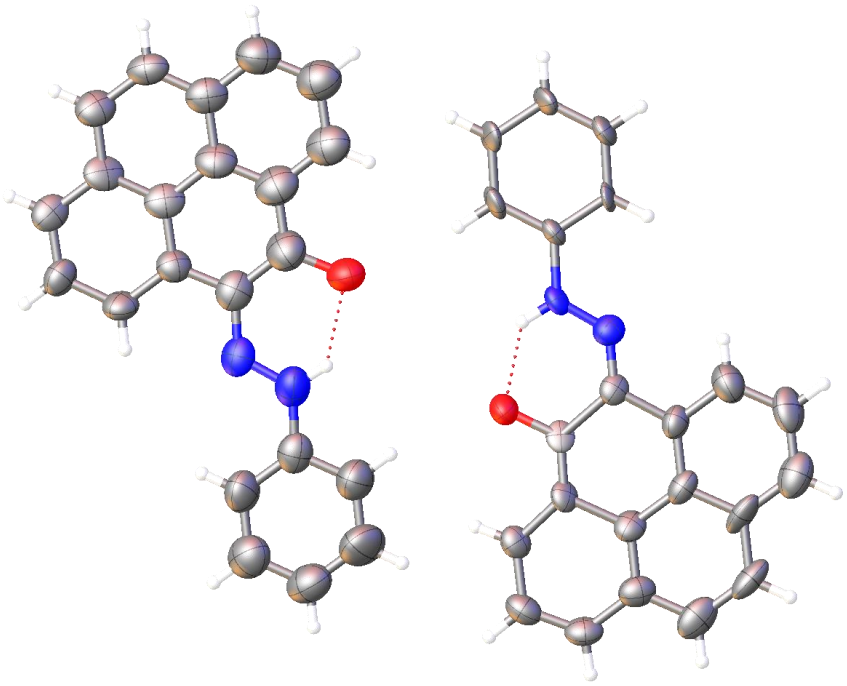

Figure S46. Molecular structure of **1** showing part 1 only. Disordered part (2nd part) is removed for clarity. Atoms are shown in thermal ellipsoids with 50% probability level.

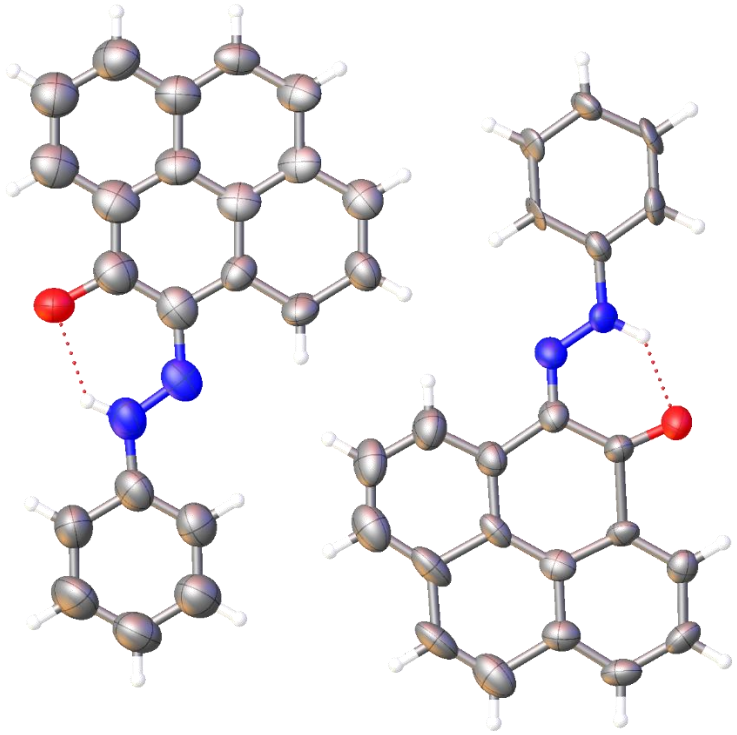

Figure S47. Molecular structure of **1** showing part 2 only. Disordered part (1st part) is removed for clarity. Atoms are shown in thermal ellipsoids with 50% probability level.

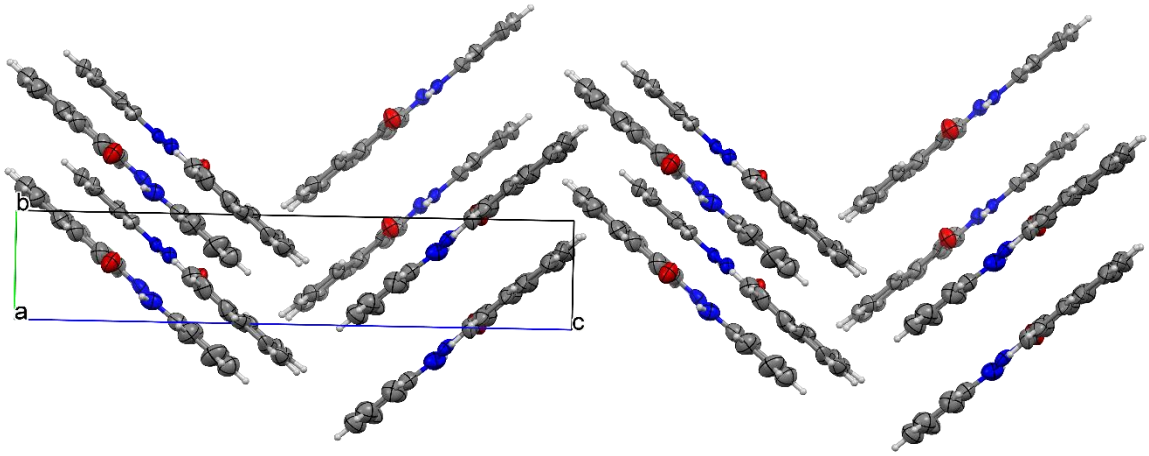

Figure S48. Packing structure of **1** (1st part only) shown along a-axis. The packing structure showed typical herringbone type packing structures due to the pyrene ring.

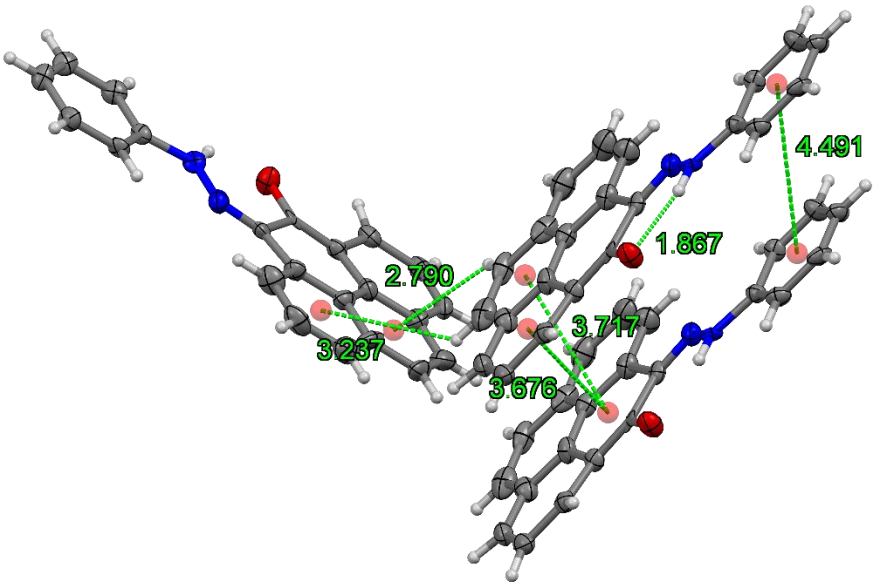

Figure S49. Different non-covalent interactions in the packing structure of **1**. The C-H•••π (2.8 – 3.2 Å) and π•••π (~3.7 Å) interactions are the main contributors for the herringbone packing.

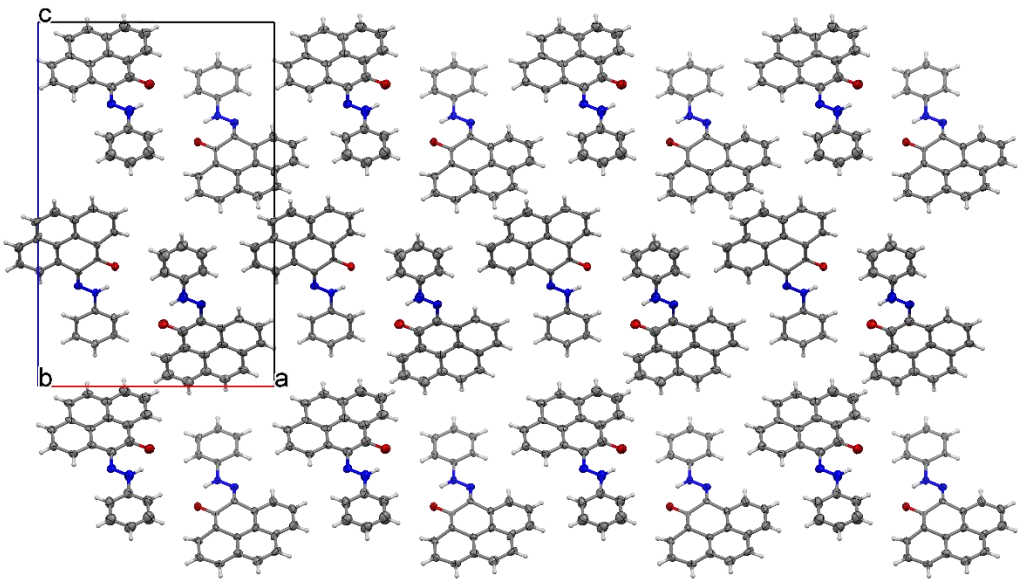

Figure S50. Packing structure of **1** (1st part only) shown along b-axis.

12. References

1. J. Hu, D. Zhang and F. W. Harris, *J. Org. Chem.*, 2005, **70**, 707–708.

2. M. N. Kumar, D. L. Lyngkhoi, S. Gaikwad, D. Samanta, S. Khatua and S. Pramanik, *New. J. Chem.*, 2023, **47**, 15066–15075.

3. G. M. Sheldrick, *Acta Cryst*., 2015, **A71**, 3–8.

4. G. M. Sheldrick, *Acta Cryst*. 2015, *C71*, 3–8.

5. O. V. Dolomanov, L. J. Bourhis, R. J. Gildea, J. A. K. Howard, H. Puschmann, *J. Appl. Cryst.*, 2009, **42**, 339–341.